Earth Systems, Resources, and Sustainability, 2026, 1(2), 221–248

Earth Systems, Resources, and Sustainability

Journal Homepage: https://www.sciltp.com/journals/esrs

Article

On the Space-Time Context of Magmatism in the Chhota Udaipur Alkaline-Carbonatite Sub-Province within the Deccan Large Igneous Province, India

Sanjeevani Jawadand[1,2] and Kirtikumar Randive[1,*]

[1] Department of Geology, Rashatrasant Tukadoji Maharaj Nagpur University, Nagpur 44001, India
[2] Shri Mathuradas Mohota College of Science, Sakkardara, Nagpur 440024, India
[*] Correspondence: randive101@yahoo.co.in

ABSTRACT

The Deccan Large Igneous Province (DLIP) represents one of Earth's most extensive continental flood basaltic events and is widely interpreted to have formed during a geologically short interval near the Cretaceous–Paleogene boundary. Within this framework, the Chhota Udaipur Alkaline-Carbonatite Sub-Province (CUACS), located in the lower Narmada rift zone, has yielded a wide range of radiometric ages, leading to suggestions of prolonged or episodic magmatism. This study integrates detailed field relationships, petrography, geochemistry, structural analysis, geophysical constraints, and critically evaluated geochronological data to reassess the spatial and temporal context of CUACS magmatism within the DLIP. The CUACS comprises diverse tholeiitic, transitional, and alkaline rock suites intruding Precambrian basement, Cretaceous sediments, and Deccan trap basaltic lava flows. Despite lithological diversity, geological relationships show no systematic cross-cutting or temporal separation among intrusive phases. Geochemical signatures indicate derivation from a common OIB-type enriched mantle source modified by crustal contamination. When evaluated in light of high-precision U–Pb and $^{40}Ar/^{39}Ar$ constraints on Deccan magmatism, the CUACS does not preserve evidence for distinct, long-lived magmatic pulses. Instead, the apparent age scatter largely reflects analytical and sampling errors. The results support a model in which CUACS magmatism is broadly coeval with the main Deccan eruptive phase, indicating short-duration magmatism for the DLIP.

ARTICLE INFO

History:

Received 8 November 2025
Revised 3 February 2026
Accepted 10 March 2026
Published: 17 March 2026

Keywords:

Deccan traps;
Chhota Udaipur;
alkaline–carbonatite magmatism;
Large Igneous Provinces;
geochronology

Citation:

Jawadand, S.; Randive, K. On the Space-Time Context of Magmatism in the Chhota Udaipur Alkaline-Carbonatite Sub-Province within the Deccan Large Igneous Province, India. *Earth Systems, Resources, and Sustainability* **2026**, *1*(2), 221–248. https://doi.org/10.53941/esrs.2026.100014

Research Highlights

- CUACS magmatism is spatially and temporally linked to the main Deccan eruptive phase.
- Apparent radiometric age dispersion reflects analytical limitations rather than episodic magmatism.
- Field, structural, and geochronological data support short-duration magmatism within the DLIP.

1. Introduction

The Deccan Large Igneous Province (DLIP) in India (Figure 1) is of global interest as one of the large continental flood basalt provinces on earth, with a horizontal stack of ∼1.5 km thick tholeiitic basaltic lava flows spreading over half a million km^2. It is bisected by several dykes and related intrusions. Alkaline magmatism associated with these rocks is volumetrically meagre, but comprises diverse rock types, including carbonatites, orangeite, lamprophyres, gabbro, nephelinites, tinguaite, and phonolite [1–6]. It has been known for the past few decades that the Deccan basaltic magmatism has occurred in a relatively short (<1 Ma) geological time span. Contrary to this view, evidences were suggested to show that the younger as well as older magmatic pulses were present in the DLIP [7–10]. Radiometric age estimates for the Deccan Large Igneous Province have been obtained through various geochronological methods, resulting in a broad spectrum of reported ages. Among these, however, only U–Pb Zircon/baddeleyite dating and ^{40}Ar/^{39}Ar analyses of carefully selected, minimally altered mineral phases can be regarded as providing reliable temporal constraints on the emplacement of LIPs. Evaluations that rely exclusively on these high-precision techniques consistently show that the main phase of Deccan volcanism occurred over a very short geological interval around ∼66 Ma, with the bulk of magma emplacement taking place within less than one million years. In contrast, the much wider age ranges reported in earlier literature are commonly attributable to analytical uncertainties, the use of altered or unsuitable samples, or the application of less precise dating methods. Recent critical reassessments of Phanerozoic Large Igneous Provinces, including the Deccan, founded solely on U–Pb and ^{40}Ar/ ^{39}Ar geochronology, therefore provide a robust basis for re-evaluating the duration and temporal evolution of Deccan magmatism [11]. These observations instigated new thinking that the Deccan magmatism could be episodic instead of a single continuous event of 0.5 to 1.0 Ma. Radiometric dating of Deccan Trap lavas and intrusions has shown that the bulk of the magmatic activities occurred at ∼65 ± 1 Ma. The volume of the lavas and associated plumbing system of dykes, sills, and layered intrusions exceeds a million cubic kilometres [12]. Based on a variety of dating techniques, few researchers have proposed that the Deccan event occurred over an extended period; possibly in pulses, at 68–60 Ma [13–19] and 65 Ma + 0.5 Ma [14, 16].

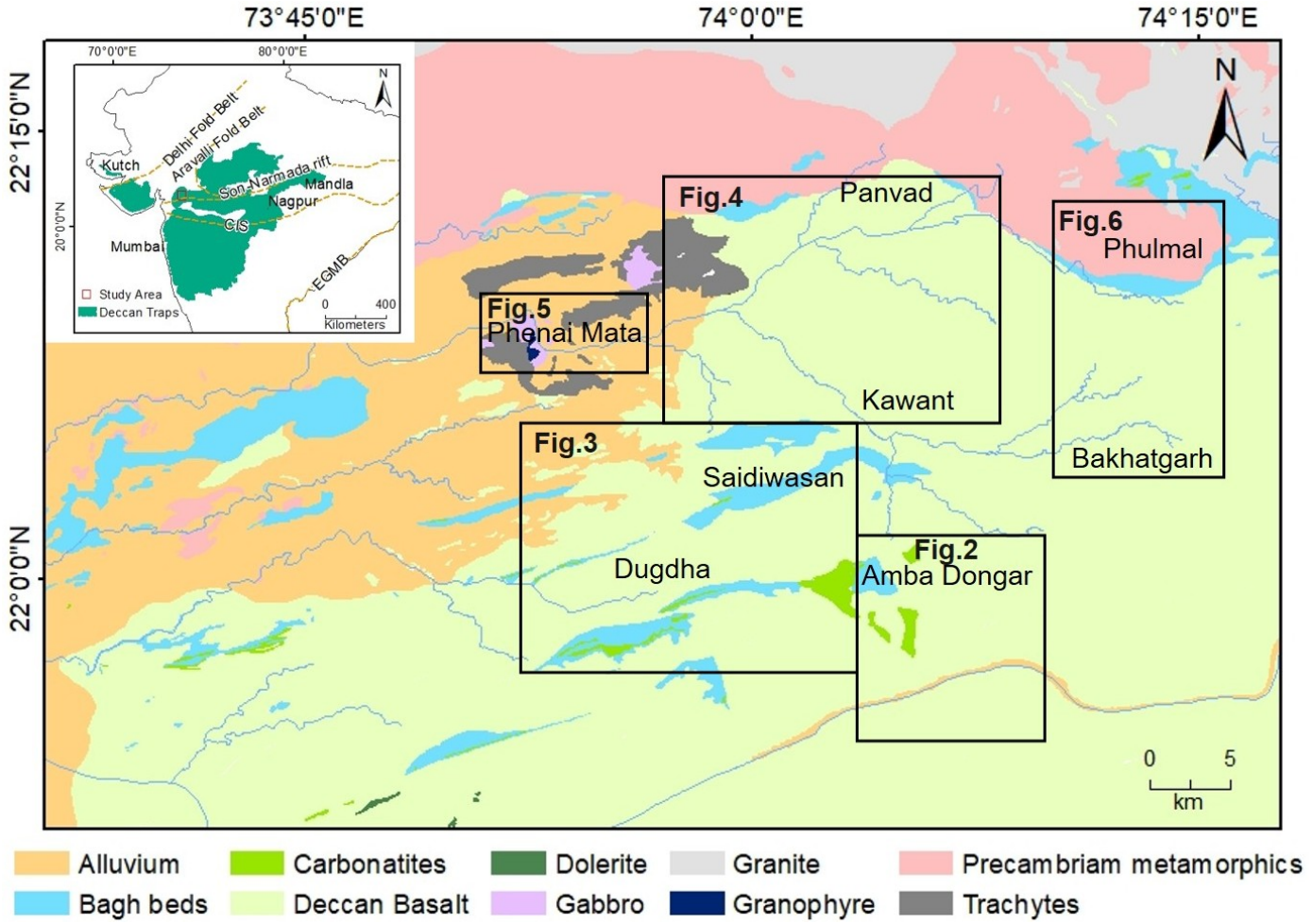

Figure 1. [Inset] Deccan Large Igneous Province. Geological map of Chhota Udaipur Carbonatite—Alkaline subprovince.

Several carbonatites and alkaline rocks are associated with the DLIP. The alkaline volcanism both preceded and followed the main Deccan magmatism [20]. The igneous intrusions that form the Island belt in northern Kutch are significantly older (^{40}Ar/ ^{39}Ar age of ∼76 Ma) than the bulk of the Deccan Traps (66 ± 1 Ma), whereas one of the intrusions in the Dhar Dongar has yielded much younger age (61 ± 0.5 Ma) [21]. However, recently Baksi [10] reviewed the age of the Deccan Traps, and after a critical assessment of the age dating techniques, he argued against any episodic magmatism in the DLIP and argued that the different ages were obtained due to flawed analytical techniques and the selection of wrong (altered) samples for analysis. In this paper, we critically examine the intrusive and extrusive magmatism in the CUACS, which has a distinct geochemical signature in comparison with other regions of the DLIP [22].

2. The Deccan Large Igneous Province (DLIP)

Large Igneous Provinces (LIPs) are commonly defined as regions of extensive mafic magmatism, typically exceeding 0.1–0.2 Mkm^2 in areal extent and emplaced over geologically short time intervals in intraplate settings with indirect links to seafloor spreading and subduction [23–26]. The Deccan Traps constitute one of the world's most significant igneous provinces (LIPs). They comprise almost 0.5 million square kilometers of area and have an initial eruptive volume of about 1.3 × 10^6 km^3 [27, 28]. The last phase of the Gondwana supercontinent's breakup occurred resulting in the Deccan volcanic eruption due to the impingement of the Reunion mantle plume [29, 30]. They comprised thick tholeiitic basalt lava piles with an exposed maximum thickness of 1700 m [31, 32]. Extensive basalt eruptions occurred from the late Cretaceous to early Eocene, with a substantial peak in activity approximately 60–65 million years ago. During this time, the Indian plate migrated rapidly northward. The eruptive centres are widely inferred to lie in the western Deccan region between present-day Mumbai (Bombay) and the Cambay (Khambhat) rift zone, based on dyke swarm geometry and plume-related reconstructions [33, 34].

The age of the flood basaltic provinces has been studied for more than 5 decades. It is now believed that most of the LIPs have erupted within a span of about ∼1 million years (e.g., Columbia River basalt [35, 36]; Parana-Etekanda basalts, [37, 38]; Siberian traps, [19, 39]. In the case of Deccan LIP, some of the recent papers indicate ∼3–4 Ma span of eruption of Deccan Trap basalts (DTB) [13, 40], whereas many others opine that the major period of eruption of the DTB is much less, i.e., ∼800 Ka [18, 41–45]. Baksi [10] has given a detailed analysis of available age data from the DLIP and questioned several spurious, wrongly calculated data and the measurements done on altered samples, and confirmed that the majority of the basaltic lava from the DLIP has erupted in a very short (<1 Ma) span of time.

The recent investigation into Deccan geochronology has markedly improved our understanding of the time frame and duration of this major igneous event. Baksi [10] meticulously re-evaluated published age data across the entire province, revealing that much of the observed age variation is attributable to analytical uncertainties and the use of altered samples. More recently, Jiang et al. [11] placed the Deccan within a global framework of Phanerozoic Large Igneous Provinces using only high-precision U–Pb and ^{40}Ar/^{39}Ar ages, reinforcing the interpretation of short-lived magmatism. Building on these studies, the present work shifts the focus to the Chhota Udaipur Alkaline-Carbonatite Sub-province, where many of the anomalous ages have been reported. By combining detailed field observations, intrusive relationships, and sector-wise geological constraints with existing geochronological data, we evaluate whether the reported age spread reflects genuine episodic magmatism or is instead an artefact of methodological and sampling limitations.

3. The Chhota Udaipur Alkaline-carbonatite Sub-province

A notable geotectonic structure in western India, the Chhota Udaipur Alkaline-Carbonatite Sub-province (CUACS) lies between 21.83°–22.28° N latitude and 73.60°–74.28° E longitude in the lower extents of the E-W trending Narmada rift valley [4, 5, 46]. The rocks of the Chhota Udaipur Sub-province show ages from Proterozoic to Recent [4, 47–50]. A large number of researchers have worked in this area, a compilation of earlier works is available in Gwalani et al. [4], Viladkar [47], and Randive et al. [48]. The Chota Udaipur area was categorized into five major sectors by Gwalani et al. [4], viz., (1) Amba Dongar, (2) Siriwasan-Dugdha, (3) Panwad–Kawant, (4) Phenai Mata, and (5) Bakhatgarh–Phulmal (Figure 1); a brief description of each of these sectors is given below.

3.1. The Amba Dongar Sector

The carbonatite-alkaline complex of Amba Dongar is a subvolcanic diatreme with a sovite ring dyke and carbonatite breccia along its inner rim. Ankeritic carbonatite forms small and large intrusive plugs in sovite, which also develops small plugs in the surrounding sandstone (Figure 2A). The fluorite mine (Figure 2(Ba)) at Amba Donger has the main host rock carbonatite (Figure 2(Bb)) and well-preserved fluorite mineralization for the next generation of enthusiasts and researchers (Figure 2(Bc)), and some of the samples kept in the GMDC guest house at Kadipani (Figure 2(Bd)). Few basalt exposures (Figure 2(Be)) occurring in Amba Dungar are also present. Sovite, sandstone, basalt, carbonatite breccia, and fenites are traversed by many thin alvikite dykes. Viladkar [47] categorizes them as phase-I and phase-II; phase-I dykes are synchronous with major intrusion, whereas phase-II dykes are younger

and intrude both sovite and phase-I alvikite dykes. The ring dyke is flanked by plugs and dykes of alkaline rocks, including nephelinite and phonolite. Thin phonolite dykes crop out within sandstone towards the north and northwest of Amba Dongar. Both the inner and outer rims of the ring dyke are covered with carbonatite breccia (Figure 2(A,Bf)). This breccia is composed of large chunks of metamorphic rocks, sandstone, basalt, alkaline rocks, and soviet. Quartz, potash feldspar, magnetite, apatite, aegirine-augite, and mica xenocrysts are also prevalent. The matrix is calcitic with a few feldspathic inclusions [4, 47].

3.2. The Siriwasan-Dugdha Sector

The Siriwasan-Dugdha sector lies between Amba Dongar and Kawant sector, starting near Siriwasan village (Figure 3A). In this locality, the Deccan Trap basalt and the E-W trending ridge comprising Bagh sediments dominate the region's undulating plain. A series of step faults striking east-west are parallel to the Narmada River [51]. The primary rock found in this area is carbonatite breccia, which was formed due to the intrusion of carbonatite through the interface between the Bagh sediments and the Deccan Trap basaltic lava flows. The geological characteristics of the Siriwasan-Dugdha area are depicted in Figure 3B, including exposures of fenitized sandstone/carbonatite breccia (Figure 3(Ba)) along the area, the fenitized gritty sandstone within the carbonatite breccia sill (Figure 3B(b,c)), conglomeratic sandstone near Mohan Fort (Figure 3(Bd)), and nodular sandstone near Mohan Fort on the Kawant-Kadipani road (Figure 3(Be)). The carbonatite breccia sill is 150 m broad and 11 km long and consists of well-developed alkali pyroxenes [51–53]. This sector has sodic and potassic fenites; the sandstone fragments are feldspathized within carbonatite breccia. Green aegirine and aegirine-augite crystals form bands within fenites [4, 51]. The central region of the sill contains a significant number of fragments of metamorphic rocks such as gneiss, schist, phyllite, and quartzite [51], as well as pools and pockets of sovite. These fragments show large variations in their sizes from a few inches to a few feet. At Padwani, angular fragments of basalt are seen [4, 54, 55]. Stratification and current bedding are evident toward the base of carbonatite breccia, where ankeritic carbonatite dominates [51].

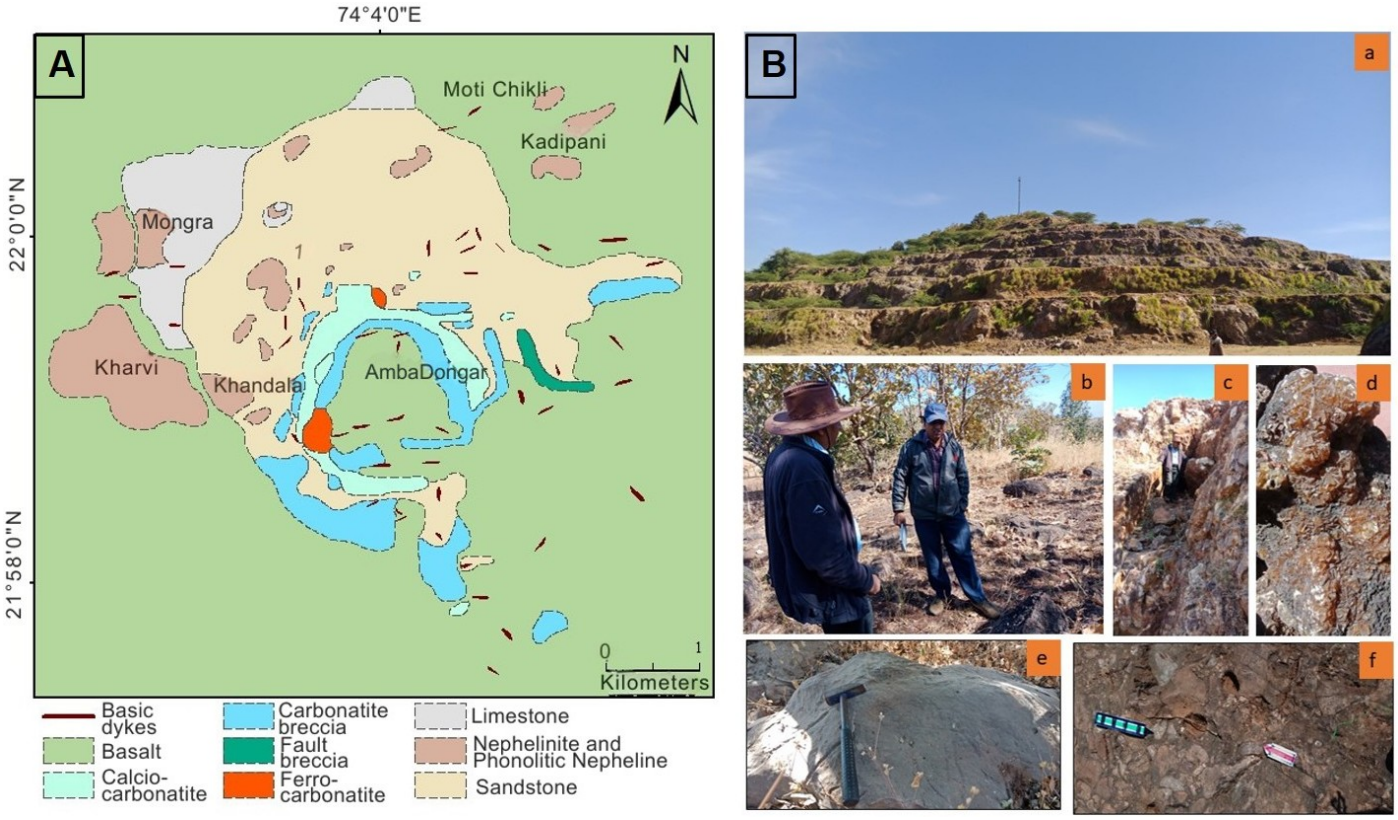

Figure 2. (**A**) Geological map of Amba Dongar. (**B**) (a) Mining benches inside the Ambadongar fluorite mine, Kadipani Tehsil, Chhota Udepur district, Gujarat; (b) A carbonatite exposure at AmbaDondar with Shri. Pandit, Scientist, AMD, Nagpur, (c) Fluorite mineralization within carbonatite at Amba Dongar, (d) A fluorite sample kept at GMDC guest house at Kadipani, (e) A basalt outcrop at Amba Dongar, and (f) An exposure of carbonatite breccia rim at Amba Dongar.

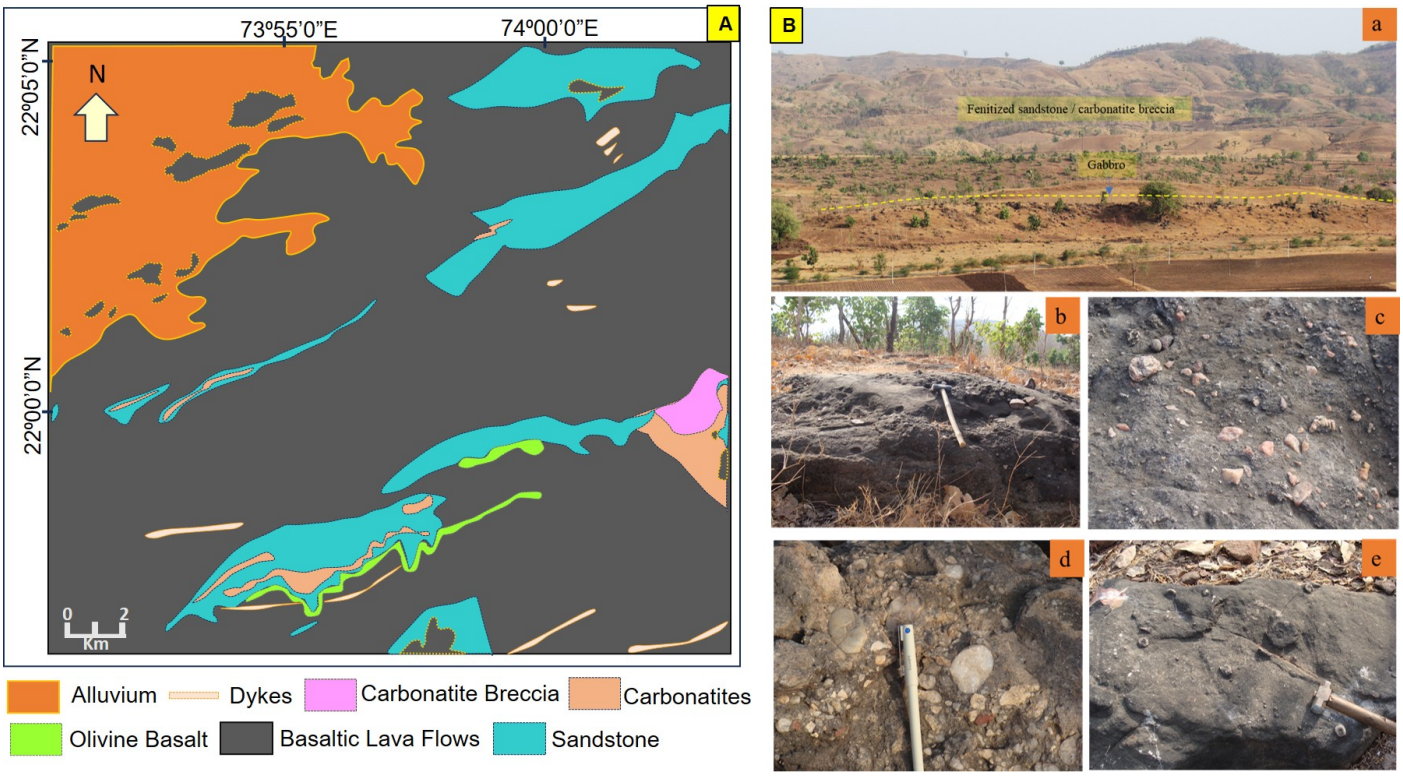

Figure 3. (**A**) Geological map of Siriwasan-Dugdha sector. (**B**) Field photograph of Siriwasan-Dugdha sector (a) A panoramic view near Siriwasan village (camera facing south) showing a linear outcrop of gabbro in the foreground, whereas the hillocks in the background showing exposures of fenitized sandstone/carbonatite breccia, (b) An outcrop of carbonatite breccia exposure near Hanuman Mandir, (c) Closer look at the fenitized gritty sandstone within carbonatite breccia sill, (d) Conglomeratic sandstone near Mohan Fort, and (e) A nodular sandstone near Mohan fort on Kawant-Kadipani road.

3.3. The Panwad–Kawant Sector

The Panwad and Kawant sector is spread between 22°5′–22°13′ N and 74°0′–74°5′ E (Figure 4A). It is characterized by varied rock types and geological features (Figure 4B), such as a prominent ijolite plug near village Kharajwat (Figure 4(Ba)), carbonatite bodies near Dungargam (Figure 4(Bb)), quartz xenocrysts laden mafic dykes (Figure 4(Bc)), lamprophyre dykes near Dungargam and nearby areas (Figure 4(Bd)), and giant pseudoleucite tinguite (Figure 4(Be)). A large number of small dykes and plugs occur in this sector, most of which are trending NW-SE and E-W. This region has a wide range of rock types, including varieties of basic, alkaline, subalkaline, and carbonatites [56]. The carbonatites occur as small dykes of alvikite and beforsite associated with carbonatite breccia [4, 57]. The dykes of carbonatite, which are dark-colored, are more ferruginous and contain patches of cryptocrystalline silica [58]. In the Panvad-Kawant area, closely associated dykes and plugs of alkaline silicate rocks are present, which include syenite, nepheline-syenite, ijolite, phonolite, tinguaites with or without giant-pseudoleucite, and lamprophyres [4, 56, 58–62] A large plug of ijolite (∼250 feet in diameter) occurs in the south of Panwad, whilst tinguaite with giant pseudoleucite phenocrysts exists near Ghori [58]. The lamprophyres comprise four types, namely kersantites, minettes, camptonite, and monchiquite [5, 56].

Some of the dykes are over a kilometer long, trending NW-SE, composed mostly of basic (dolerite and basalt), alkaline (tinguaite, pseudoleucite tinguaite, ijolite, lamprophyres), and carbonatite (sovite and alvikite). The smaller dykes tend ENE-WSW and E-W (some relatively bigger dykes near Panwad also follow this trend) and these are composed of basic (basalt, dolerite, and gabbro) and alkaline rocks (nephelinite, tinguaite, phonolite, and nepheline syenite). Minor dykes follow the trend of the Heran and Kara rivers, which are fault zones [4, 56, 57]. There are some enigmatic quartz-xenocrysts laden dykes near Rorda and Samalawat [50, 63, 64].

3.4. The Phenai Mata Sector

The Phenai Mata (Figure 5(A,Ba)) is a bimodal igneous complex with tholeiitic and alkaline magmatism and was previously considered to be a differentiated complex comprising basalt, gabbro, diorite, nepheline-syenite, lamprophyre, and granophyre [62, 65–67]. Basalt makes up three-quarters of PMIC, while felsic rocks and gabbro make up the remaining one-third. The eastern side of the hill is dominated by felsic rocks, whereas the northeastern side is dominated by gabbroic rocks. There are

two distinct types of gabbro viz., (i) tholeiitic gabbro which is closely related to tholeiitic basalt and acid differentiates, and (ii) alkali gabbro which is closely associated with syenitic rocks located in the north-northeast portion of Phenai Mata hill. This rock shows layering formed due to cumulates of pyroxene and olivine [62, 68–71]. A tholeiitic gabbro displays variation from gabbro (sensu stricto), olivine gabbro, leuco-olivine gabbro, mela-olivine gabbro, anorthosite, and troctolite; whereas an alkali gabbro displays variations such as mela-olivine gabbro and plagioclase-containing pyroxenite [71]. On the southern side of the Heran River, there is an outcrop that exposes a large anorthosite plug [4, 59, 60]. A few, lamprophyre, breccia dykes (Figure 5(Bb)), aphyric dykes (Figure 5(Cc)) and dolerite dykes occur within basaltic lava flows and layered gabbro (Figure 5(Dd)) [4, 71–74].

Gwalani et al. [4, 57] observed a layered tholeiitic gabbro-granophyre intrusion with a nepheline syenite plug and tephrite, phonolites and lamprophyre dykes in the PMIC. The region has both undersaturated and oversaturated syenites. A small dyke of quartz-bearing microsyenite intrudes through coarse-grained nepheline syenite [4, 57, 62, 68, 69, 71, 72]. Microgranites are pink, porphyritic, and rich in pyroxene and amphibole. The granophyre resembles microgranite and is difficult to distinguish macroscopically [62, 68, 69, 71, 75].

3.5. The Bakhatgarh–Phulmal Sector

Bakhatgarh–Phulmal sector (Figure 6A) is one of the five sectors of the Chhota Udaipur alkaline-carbonatitic sub-province, identified by Gwalani et al. [4]. The major rock types occurring in this area include Precambrian quartz-mica-schist, Cretaceous Bagh sediments, and Upper Cretaceous to Lower Eocene Deccan Trap basaltic lava flows and dykes (Figure 6B). The intrusive dykes follow three distinct structural trends, viz. EW, NE-SW, and ENE-WSW, which are in concurrence with the E-W trend of the Narmada lineament (e.g., Deshmukh and Sehgal, [76]). These dykes were grouped into four distinct types, viz. (1) picrobasalts (Figure 6(Ba)); (2) lamprophyres such as minette, karsentite, camptonite, and monchiquite; (3) tholeiitic comprising basalt, dolerite, gabbro, porphyritic basalt, and giant plagioclase basalt; and (4) Calcareosiliceous dykes (Figure 6(Bb)) represented by carbonate breccias, calcite, and quartz dykes and veins [5, 77]. These are dyke-like bodies with an E-W trend, composed of calcite, quartz, and cryptocrystalline silica matrix often coated with limonite staining. These dykes or reefs have slicken-sides on both surfaces [5, 78]. The lamprophyre dykes exhibit porphyritic–panidiomorphic texture even at the outcrop scale (Figure 6(Bc)). Similarly, ocelli structure (Figure 6(Bd)) and presence of xenoliths (Figure 6(Be)) is often seen in the picrobasalt and lamprophyre dykes.

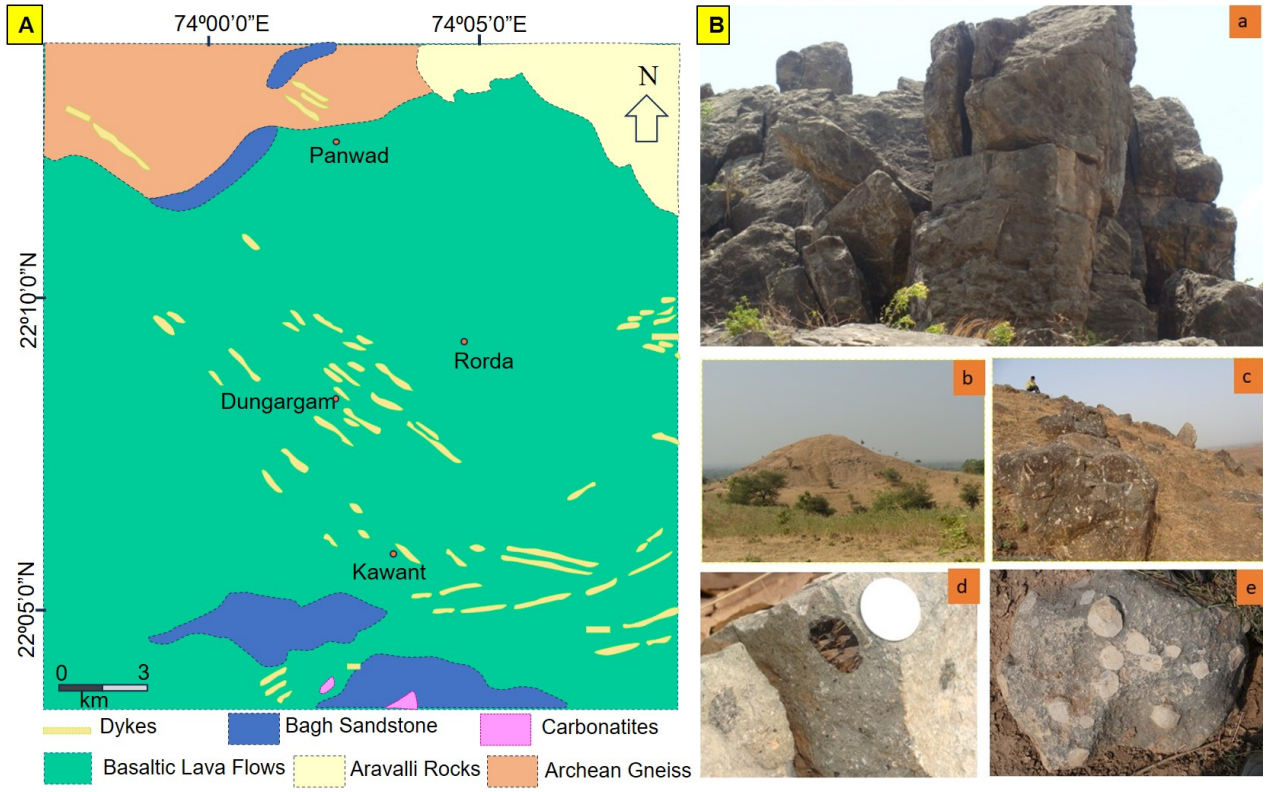

Figure 4. (**A**) Geological map of Panwad–Kawant sector. (**B**) Field photographs from Panwad–Kawant sector (a) An ijolite plug near village Kharajwat, (b) A conical hill showing fenitized basalt (a carbonatite plug) near Dungargam, (c) A quartz xenocrysts laden mafic dykes near village Rorda, (d) A lamprophyre dyke near Dungargam showing rounded mica phenocryst and other xenoliths and (e) An exposure of giant pseudoleucite tinguite dyke.

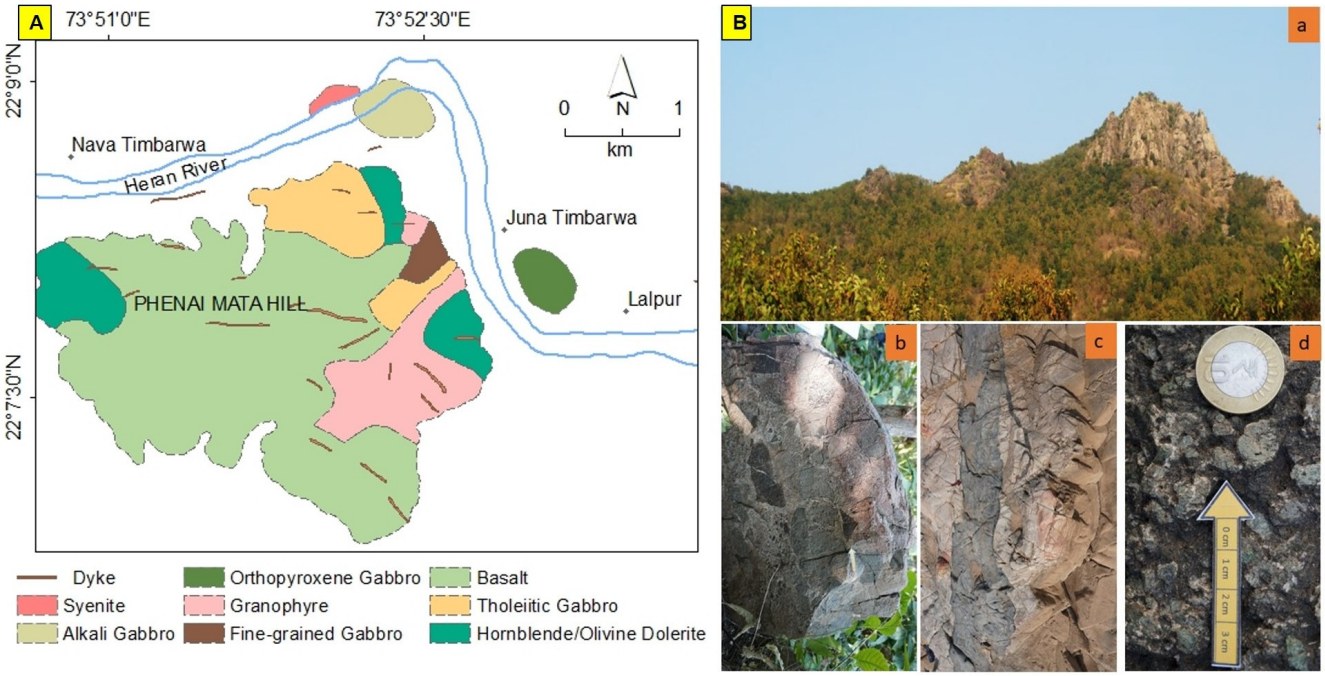

Figure 5. (**A**) Geological map of Phenai mata. (**B**) Field photographs from the Phenai Mata sector (a) Panoramic view of the Phenai Mata dungar (hill). Mostly granophyre is exposed along this side (camera facing towards north), (b) An exposure of a breccia dyke atop Phenai Mata hill, (c) An aphyric dyke intruding through in near Phulbai Mata temple, and (d) An outcrop of a cumulate gabbro showing phenocrysts of olivine and pyroxene (greenish hue).

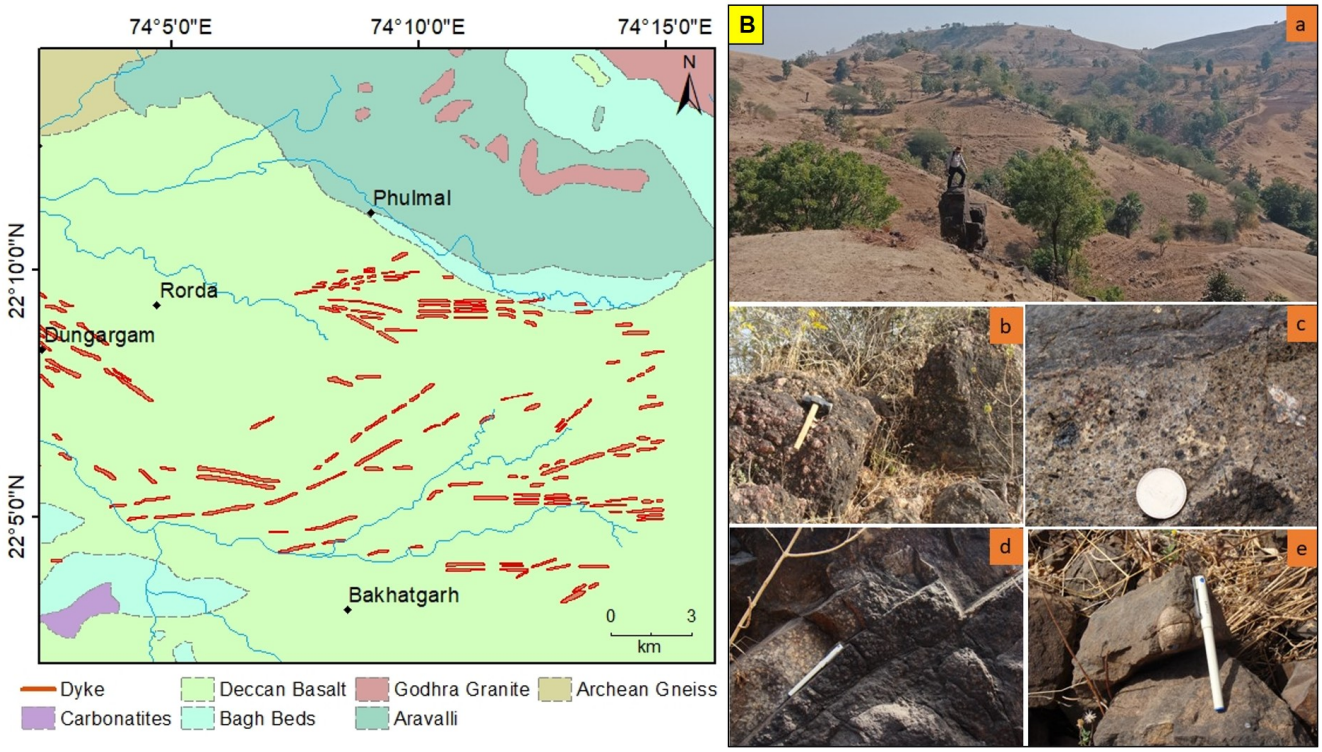

Figure 6. (**A**) Geological map of Bakhatgarh–Phulmal sector. (**B**) Field photographs from Bakhatgarh- Phulmal sector, (a) A panoramic view of dykes exposed near village Undri, (b) An exposure of a calcareosiliceous dyke near Chhaktala, (c) A close view showing porphyritic texture in a picrobasalt exposed on one of the hillocks around the Bakhatgarh area, (d) Exposure of lamprophyres on top of hillock around the Phulmal area showing ocelli, (e) A lamprophyre dyke containing rounded xenolith near Phulmal.

4. Petrography of Selected Rocks

There is a great diversity of rocks occurring in the Chhota Udaipur Alkaline-Carbonatite Sub-Province, ranging from tholeiitic basalts and gabbros to alkaline silicate rocks, lamprophyres, picrobasalts, and carbonatites. Detailed petrographic descriptions of individual lithologies are provided in key published studies and are therefore not repeated here. For e.g., detailed petrography of the carbonatite has been given in the pioneering studies of Sukheswala and Avasia [56], and Sukheswala and Borges [51]. Similarly, detailed petrography of alkaline rocks is given by Sukheswala and Sethna [58], Gwalani et al. [4, 57], and Viladkar [7]. The lamprophyres were described by Hari et al. [78], Randive [5, 79, 80], and Pandey et al. [81]. The gabbro of the Phenai mata area were discussed by Vijaya Kumar and Randive [22], Hari et al. [67], and Randive et al. [74]. The syenites of the Phenai mata area were discussed in detail by Hari et al. [82]. Similarly, the trachytes and basalts of the Dugdha-Naswadi area have been described so far only by Gwalani [53], and Gwalani et al. [4, 57]. The petrography of picrobasalt, lamprophyre, basalt, and dolerite dykes of Bakhatgarh–Phulmal have been described by Randive [5] and Randive [79]. All the literature cited above provides a wealth of information about the petrography of various rock types occurring in the Chhota Udaipur region. Representative varieties of rocks from all the three rock series, such as, tholeiitic (gabbro and basalt varieties), calc-alkaline (picrobasalt and lamprophyre), and alkaline (ijolite, pseudoleucite tinguaite) are discussed below.

4.1. Tholeiitic Series

Gabbro and basalt for the part of tholeiitic series. The exposures of gabbro are found all over the CUACS, the prominent exposures are found in the Phenai Mata and Siriwasan Dugdha and Panwad–Kawant areas. Tholeiitic and alkali gabbros exhibit a variety of cumulate textures. The mineral composition of tholeiitic gabbro largely corresponds to gabbro [83], olivine gabbro, leuco-olivine gabbro, mela-olivine gabbro, anorthosite and troctolite; whereas, alkali gabbro belongs to mela-olivine gabbro and plagioclase bearing pyroxenite. In thin section, it exhibits coarse-grained holocrystalline texture, comprises of feldspar (plagioclase), sub-ordinate to minor amounts of olivine and minor to very minor amounts of pyroxene, mica (biotite), amphibole, quartz, magnetite and ilmenite (Figure 7a–d). Pyrite, chalcopyrite, sphalerite, galena, hematite and goethite/limonite are found in traces.

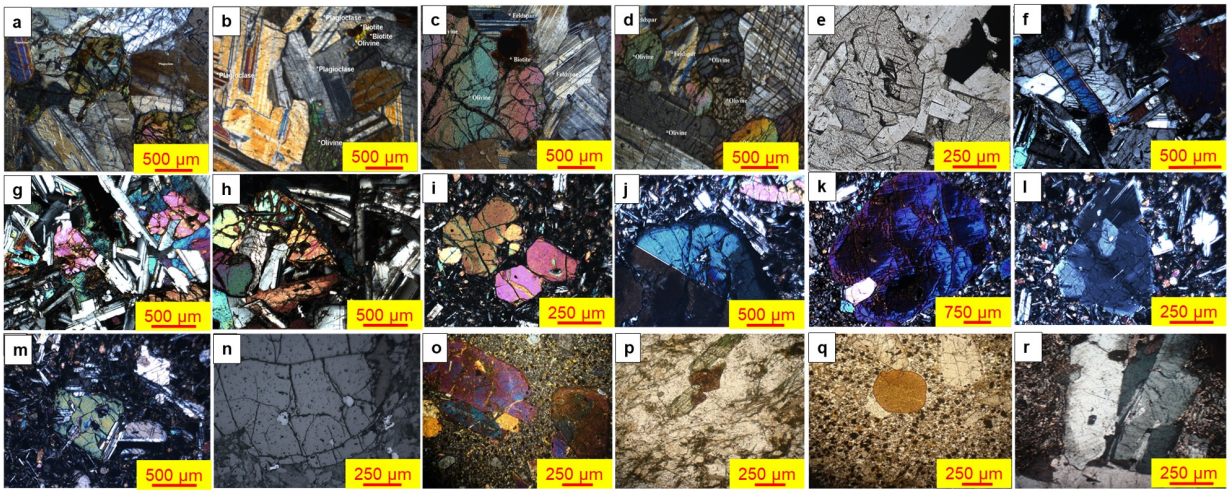

Figure 7. Photomicrograph showing (**a**) Coarse-grained holocrystalline texture in gabbro. Lath-shaped (elongated) plagioclase grains exhibiting lamellar twinning. Olivine grains are surrounded by plagioclase phenocrysts. Alteration of olivine to brownish-coloured iddingsite along the cracks and fracture planes and grain boundaries, (**b**) The assemblage of plagioclase feldspars, olivine and biotite. Lamellar twinning of plagioclase feldspars is distinct and preponderant, (**c**) Olivine grains show alteration along the irregular cracks, fracture planes and grain boundaries. Olivine phenocrysts are surrounded by the plagioclase feldspar, and (**d**) Subhedral-shaped olivine grains are surrounded by plagioclase phenocrysts. Olivine grains carry minute inclusions of opaque minerals, (**e**) Clinopyroxene with 2-sets of cleavage (5X), (**f**) Clinopyroxene and plagioclase phenocryst, (**g**) Alteration of olivine along cracks and fracture, (**h**) Interstitial olivine (**i**) Olivine cumulates embedded in a fine-grained matrix (5X), (**j**) Zoned olivine crystal (5X), (**k**) Clinopyroxene phenocryst in 2.5X showing inclusion, (**l**) Zoned plagioclase crystal (5X), (**m**) Plagioclase laths in olivine (10X) (**n**) Olivine with chromite inclusion in reflected light (10X) (**o**) Panidiomorphic texture in lamprophyre of Dungargam area. Idiomorphic phenocrysts of clinopyroxene and olivine mica are embedded within fine-grained (often glassy) groundmass composed of olivine, pyroxene, mica, spinels, and plagioclase (5X Crossed Polars), (**p**) Phenocrysts of aegirine and aegirine-augite, less commonly kaersutite, with complete pseudomorphs of olivine. Innumerable tiny needles of pyroxenes and amphiboles are seen. The groundmass shows the growth and abundance of feldspars (plagioclase and potash) and feldspathoids (5X Plane Polars), (**q**) Zoned pyroxenes and rounded mica phenocryst (5X Crossed Polars), (**r**) Plagioclase megacryst in ocelli within the groundmass.

The basalts are porphyritic as well as non-porphyritic (Figure 7e–n). The porphyritic basalts are further classified using the classification proposed by West [84], as three-phenocryst basalt—3PB (olivine, clinopyroxene and plagioclase); two-phenocryst basalt—2PB (either olivine and plagioclase or pyroxene and olivine); one-phenocryst basalt—1PB (one phenocryst of plagioclase feldspar); and giant plagioclase basalt—GPB (big laths of plagioclase ranging in size from 1 to 5). All of the phenocrysts are well defined (idiomorphic), and formed independent of one another (porphyritic); they also sometimes formed in clusters (glomeroporphyritic). The groundmass invariably contains these three minerals along with magnetite and glass. Deuteritic alteration is prominent; similarly, secondary calcite, quartz and Fe oxides also occur.

4.2. Transitional Series

The lamprophyre and picrobasalt form the part of transitional series, which are discussed here. The Lamprophyres are characterized by porphyritic–panidiomorphic texture and the presence of hydrous minerals, either as phenocrysts or in groundmass or both. On the basis of mineralogy and texture, Gwalani et al. [4], Hari [78], Randive [5], and Chalapathi Rao et al. [46] previously classed lamprophyres from the Chhota Udaipur region as alkaline and calc-alkaline. The lamprophyres are fresh, exhibit well-preserved porphyritic and panidiomorphic texture (Figure 7o–r). Common phenocrysts are olivine, clinopyroxenes, mica, and amphibole. Clinopyroxene (diopside, augite) phenocrysts are most abundant, followed by rounded to subrounded olivine showing resorbed grain boundaries and development of serpentine along the fractures. Mica phenocrysts are rounded in shape with corroded borders. Groundmass contains innumerable (<1 mm) opaques (magnetite/ulvospinel), tiny needles/laths of mica and clinopyroxene, and abundant tiny plagioclase crystals.

Picrobasalt is porphyritic in nature, fine-grained and has large and abundant phenocrysts of olivine and pyroxene, with relatively less or occasional occurrence of plagioclase phenocrysts. The groundmass comprises of iron oxides, apatite, fluorite analcime (accessory minerals), carbonates, serpentine and iddingsite (altered mineral phases). The porphyritic to panidiomorphic texture is very prominent, where phenocrysts are dominant of pyroxene with subordinate nepheline (Figure 8a–f). Groundmass also consists of nepheline, plagioclase feldspar, biotite, and chlorite (mica which is altered). The pyroxene occurs as a phenocryst as well as microcryst; predominantly euhedral in shape with resorbed grain boundary at places.

Olivine phenocrysts in picrobasalts are idiomorphic with sharp crystal boundaries and form large (0.2–0.5 mm) angular though irregular resorbed grains due to magmatic corrosion and partial resorption. It occurs as independent crystals as well as in clusters. Olivine is altered partially or completely along the cracks or fracture zones. Plagioclase occurs both as a phenocryst and in the groundmass. It occurs as lath-shaped and shows polysynthetic twinning, the twin individuals being of unequal width. Pyroxenes are mainly of augite (clinopyroxene) in composition present both as subhedral phenocryst and in groundmass. It is faint pinkish in colour, non-pleochroic and rarely shows the development of prismatic cleavage. Biotite in groundmass shows pleochroism and at places, it is altered to chlorite. Magnetite forms dusty inclusions and shows inhomogeneous distribution throughout the rock. It covers ∼10% volume of the rock composition along with other opaques. Apatite is present as an inclusion within some minerals or in glass (Figure 8a–f).

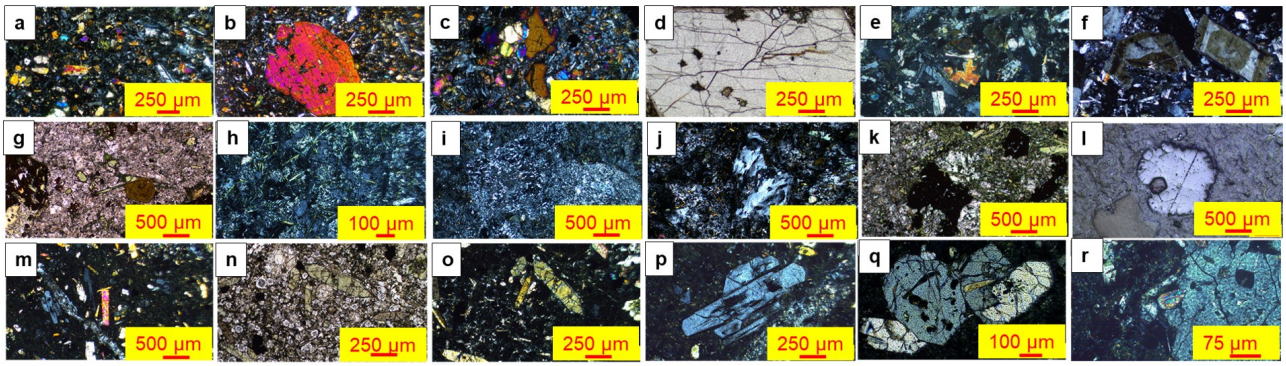

Figure 8. Photomicrograph showing (**a**) Plagioclase, olivine and pyroxene embedded in the groundmass of picrobasalt (2.5X), (**b**) Olivine phenocryst showing alteration along cracks (2.5X), (**c**) Resorbed olivine grain (2.5X), (**d**) Hexagonal pyroxene crystal showing inclusion (2.5X), (**e**) Biotite in groundmass altered to chlorite (20X), (**f**) Zoned pyroxene/leucite crystals (10X)′ Photomicrographs (2.5X) showing (**g**) Microporphyritic texture in pseudoleucite tinguaite, (**h**) Green-coloured aegirine needles distributed throughout the groundmass, (**i**) Pseudoleucite (**j**) White-grey coloured nepheline crystals in rectangular form, (**k**) Fe-oxide with aegirine embedded in GM matrix (**l**) Pyrochlore in reflected light, Photomicrograph showing (**m**) Nepheline, magnetite with altered leucite (2.5X), (**n**) Embedded green-coloured aegirine crystals in PPL (5X), (**o**) Elongated aegirine-augite crystals with sharply pointed terminations (5X), (**p**) Nepheline crystal (10X) (**q**) Twinned clinopyroxene (10X), (**r**) Inclusion of zircon (10X).

4.3. Alkaline Series

The carbonatite alkaline rocks are the major components of alkaline series of rocks. Different varieties of carbonatite such as sovite, ankeritic carbonatite, alvikite, as well as extrusive phases occur in the area. Carbonatites are extensively studied and discussed previously, for e.g. Viladkar [47, 61]. Therefore, not discussed here further. A variety of alkaline rocks occur in this area. The pseudoleucite tinguaite is an alkaline rock composed of fine-grained euhedral (trapezohedral) pseudoleucite megacrysts along with K-feldspar, aegirine-augite, nepheline, pyrochlore and Fe-oxide. Phenocrysts of nepheline are greyish-blue and square-shaped (Figure 8g–l).

A prominent exposure of ijolite is present near Kharajwant in the Panwad–Kawant sector. This intrusive igneous rock occurs as a large plug in the field. It is holocrystalline essentially composed of clinopyroxene (aegirine-augite) and nepheline. Green-coloured aegirine augite shows pleochroism distributed throughout the groundmass (Figure 8m–r).

5. Interrelationships between the Cuacs Rocks

The field data and physical relationships between the geological features were used to assess their relative ages and to describe an age relationship of broader geological features. The criteria and rationale for using them are given below.

5.1. Geological Relationships Inferred from Spatial Patterns

A detailed geological map of the Chhota Udaipur alkaline-carbonatite sub-province (CUACS) is given by Gwalani et al. [4], which was mapped between 1963 and 1986 by Sukeshwala and coworkers. This compilation is the only compilation available of the Chhota Udaipur intrusive complex, wherein the space-time relationship between various rocks was proposed. According to these workers following rocks or group of rocks are present in the area, from oldest to youngest: (i) The Precambrian Metamorphic rocks including quartzite, quartz-mica schist, granitic gneiss and granite belonging to the Aravalli Supergroup, (ii) The sandstone and limestone belonging to Cretaceous Bagh sediments, (iii) The basaltic lava flows of the Deccan trap magmatic episodes, which are punctuated by an intertrappean green bole, red bole and ash beds, (iv) Intrusions of trachyte within the lava flows [53], (v) The intrusive complex of Amba Dongar comprising of three major rock types, namely, older alkaline rocks (tinguaite, nephelinite and phonolite), carbonatite breccia, carbonatites and the younger calcareo-silicious rocks, (vi) The alkaline-carbonatite suit of rocks is followed by younger Phenai Mata tholeiitic complex, which is comprised of (from older to younger) anorthosite, layered gabbro/gabbro, hornblende dolerite and granulitic dolerite, basalt, epidiorite, pulaskite and granophyre, and (vii) The youngest of all was considered to be the dykes and plugs of alkaline, basic, carbonatite and picritic basalt.

The Precambrian metamorphic and Cretaceous sedimentary rocks are undisputedly older. The lava flows have shown intense calcitization, so much that, at some places, altered basalt became the ‘plagioclase calcite rock’ due to replacement of mafic minerals by calcite and remnants of plagioclase in the rock [56]. Similarly, the uralitization of pyroxenes and presence of epidote led Sukheswala and Avasia [56] to name this altered rock as an ‘epidiorite’. These effects are possibly due to the influx of hydrothermal fluids. In the Amba Dongar area, basalt is present both outside the ring dyke as well inside the ring dyke, making it unclear to assign a younger or older status to carbonatite than basalt [46, 77]. Similarly, the intrusive suite of dykes that were considered as younger as compared to other sectors have been dated precisely at ∼65 Ma (see Discussion). There is no direct evidence of the PMIC suit being younger or older than the carbonatites and alkaline rocks of Amba Dongar sector. The same is the case with lamprohyre and picrobasalt dykes of Bakhatgardh–Phulmal sector, which do not show cross-cutting with other intrusive rocks of the nearby Panwad–Kawat sector. On the whole, the mapping pattern does not show any evidence of age difference among the rocks of the CUACS.

5.2. Linear Structures

Linear structures such as fractures, joints, and faults can provide information about their relative ages. We identified lineaments by combining detailed field mapping, reviewing published geological maps of the area, and interpreting satellite images and digital elevation data. Based on their continuity, orientation, and field expression, linear features that correspond to faults, fractures, dykes, and prominent geomorphic lineaments were mapped. After that, ground observations were used to check these lineaments wherever possible.

5.2.1. Faults

The CUACS has a strong imprint on the structures that are the artefact of the major Narmada lineament (rift valley). Sukeshwala and coworkers have reported a series of step-faults which were formed consequent to Narmada rifting (parallel) and offsetting (perpendicular) to the E-W trending structural grain of the Narmada lineament zone [4]. In this area, two distinguishing trends along the NNE-SSW and ENE-WSW marked by the oblique faults cross-cutting at 120° are seen. It is apparent that both sets of faults are contemporaneous. The dykes have exploited both the fault planes. Although the dykes appear to show opposing trends, they are unlikely to be of different ages.

5.2.2. Joints and Fractures

There are at least three sets of joints/fractures, viz., E-W, NW-SE, and ENE-WSW trending. Apart from these trends, occasional branching of the lineaments is observed. They appear to show cross-cutting; however, the dykes and veins exploiting these joints/fractures do not show cross-cutting in the field. This reiterates that the

materials exploiting these planes do not belong to the different magmatic events.

5.2.3. Dykes

There is a plethora of dykes present in the CUACS. They vary in composition and the trend in which they occur. Their map pattern is suggestive of their possible cross-cutting, but their direct contacts in the form of such as chilled contacts, truncation of one against another, dislocation, enduring-fritting-burning effects, etc., are missing on the ground. The lamprophyre, picrobasalt, alkaline rocks, and carbonatite dykes' trend along the NW-SE direction, which stands against the ENE-WSW trending, calcareosiliceous dykes.

Similarly, a few E-W trending picrobasalt and lamprophyre dykes are observed near Kanthari, Biswani, Undri, and towards Bakhatgarh. Nevertheless, no direct cross-cutting of dykes is observed in the field. At some places such as Dhorat and Kanthari, a calcareosiliceous dyke appears to cut across a 2PB dyke (Figure 9a), and near Dungaragam, a lamprophyre dyke (Figure 9b). Based on these evidences, it is possible to postulate that the calcareosiliceous dykes are relatively younger. However, the geochronological evidences are required to know the proper age of the calcareosilicious dykes in order to determine their position and bearing on the genesis of the CUACS.

Figure 9. (**a**) Possible cross-cutting between calcareosiliceous and 2 PB dyke near Dhorat village, (**b**) An intrusion of a lamprophyre dyke in gabbro near Dungargaon, (**c**) A mafic xenolith in an alkaline rock, (**d**) A leucocratic xenolith in a gabbro near Phulbai Mata temple, (**e**) A felsic xenolith in a lamprophyre dyke near Kundwath, (**f**) A synplutonic dyke in the Phenai Mata region. The dyke shows irregular and curvy outlines, (**g**) Felsic segregation showing hybridization in a lamprophyre dyke near Panwad, and (**h**) A lamprophyre dyke interfingering with calcareosiliceous rock near Dungargam.

5.2.4. Relationship between Faults, Joints/Fractures and Dyke Emplacement

The CUACS area is one of the major centers of dyke emplacement and an epicenter of tectonic activities. The Narmada River is a rift valley comprised of a series of step-faults, formed along two dimensions, i.e., E-W trending extensional faults and N-S trending offsetting faults. However, the intrusion of a ring dyke at Amba Dongar and other intrusive centers such as Phenai Mata, Dungargam, Rajawat, and Biswani have also opened up several joints and fractures in the area. There is a great diversity in the composition of the dykes. Although these dykes occur along the three structural trends discussed earlier, there is no evidence that a particular trend is followed by a dyke of a particular composition. However, in general, the following observations are made. (i) The lamprophyre and picrobasalt occur along NW-SE as well as E-W trends, (ii) The dolerites, 2PB, 3PB, and Giant Phencocrysts Basalt (GPB) dykes occur mostly follow E-W and ENE-WSW trends, and (iii) The calcareosiliceous dykes occur along the ENE-WSW trend. Notwithstanding the above, several smaller calcareosiliceous dykes, calcite, and quartz veins are randomly oriented. The plane of weakness formed in this region is related to the rifting event and the emplacement of dykes along such planes. The occurrence of dykes of similar composition along different structural grains indicates that they are coeval and contemporaneous.

5.2.5. Xenoliths

The xenoliths of older rocks can occur within younger intrusive rocks; such xenoliths provide important clues about the temporal difference between them. However, xenoliths are not very common in the CUACS (e.g. Figure 9c–e). Randive [80] has recorded the presence of crustal xenoliths in picrobasalt and lamprophyres in CUACS. Hari and Randive [73] have recorded several xenoliths within PMIC gabbro. A number of xenoliths are present in the calcareosiliceous dykes [4, 5, 78] as well as carbonatite breccias [4]. The quartz xenocrysts-laden dykes have profuse quartz xenocrysts [50, 63, 64]. The xenoliths occurring in breccia and calcareosiliceus dykes are comprised of older metamorphic rocks and sedimentary rocks (sandstone and limestone). There is no evidence of occurrence of one type of intrusive rock into another.

5.2.6. Chilled Margins

The time difference between various rocks can also be indicated by the chilling effect of hot, younger magmatic rocks on the old, colder rocks. Different magmatic pulses allow the preservation of internal chilled margins and the development of near-rigid surfaces at their contacts, increasing the alignment and clustering of crystals during magma replenishment [85]. Therefore, the presence of chilled margins can provide some information on the relative ages of the rocks. There are a number dykes emplaced within gabbro at Phenai Mata; however, these are synplutonic dykes having irregular, curvy, and concave margins (Figure 9f). They show changing trends due to plasticity or low rigidity of the hosts, indicating mixing and mingling of magmas [73]. However, chilling effects are seen along the margin of several smaller dykes and veins on the country rocks such as basaltic lava flows and occasionally sandstone. On the other hand, some of the dykes are mixed, multiple and some show branching, for e.g. an alkaline and lamprophyre dyke near Panwad, felsic segregation showing hybridization in a lamprophyre dyke near Panwad (Figure 9g), a dykelet within small dyke near Titod, and branching of a lamprophyre dyke near Dungargam (Figure 9h). The multiple dykes, differentiated dykes or the branching within a dyke belong to the same magmatic episode in the CUACS.

5.3. Geophysical Evidence

Singh et al. [86] have presented a detailed geophysical structure of the Phenai Mata complex based on gravity and magnetic anomalies and also interpreted their relative ages based on these data and comparison with other areas of the DLIP. They observed the presence of a mafic body of density 2.86 gm/cm^3, having a bipolar magnetic anomaly varying from -800 nT to 1200 nT. The paleomagnetic measurements of olivine gabbro and syenites of the PMIC have indicated reverse magnetization with magnetic inclination (I) of $\sim 44^\circ$ and declination (D) of 160° (see Figure 10a,b). Based on these data, these authors opined that the magnetic polarity of the PMIC was intruded during the 29R magnetic episode at the end phase of the Deccan magmatism [86, 87]. Earlier workers, notably, Vandamme et al. [88] have shown that the Deccan lava flows show 29N-29R-30N (NRN) sequence; whereas, Pande et al. [13] and Verma and Khosla [89] have concluded that the Deccan magmatism concluded between 31R and 28N magnetic chron, indicating an episodic magmatism from $\sim$69 Ma to $\sim$63 Ma (Figure 10c). However, it was shown by Baksi [90, 91] that these ages have an error due to inhomogeneous standards used in their analyses. Moreover, it is clearly demonstrated that the PMIC area preserves the remnant magnetization corresponding to 29R only [86], reiterating that the magmatism in the CUACS is restricted within a narrow time period, unlike proposed by earlier workers, e.g. Pande et al. [13].

The figures 10a,b, and c were redrawn schematically using the geological and geophysical descriptions and published sketch maps from Singh et al. [86] to ensure originality while maintaining scientific accuracy. The models and chronologies were recreated manually using vector-based tools, preserving the relative proportions, lithological units, and physical parameters (density and magnetization) reported in the original publication. These schematic reconstructions are intended to illustrate the interpreted subsurface geometry and temporal relationships of the Phenai Mata igneous complex, without reproducing original numerical datasets or imagery.

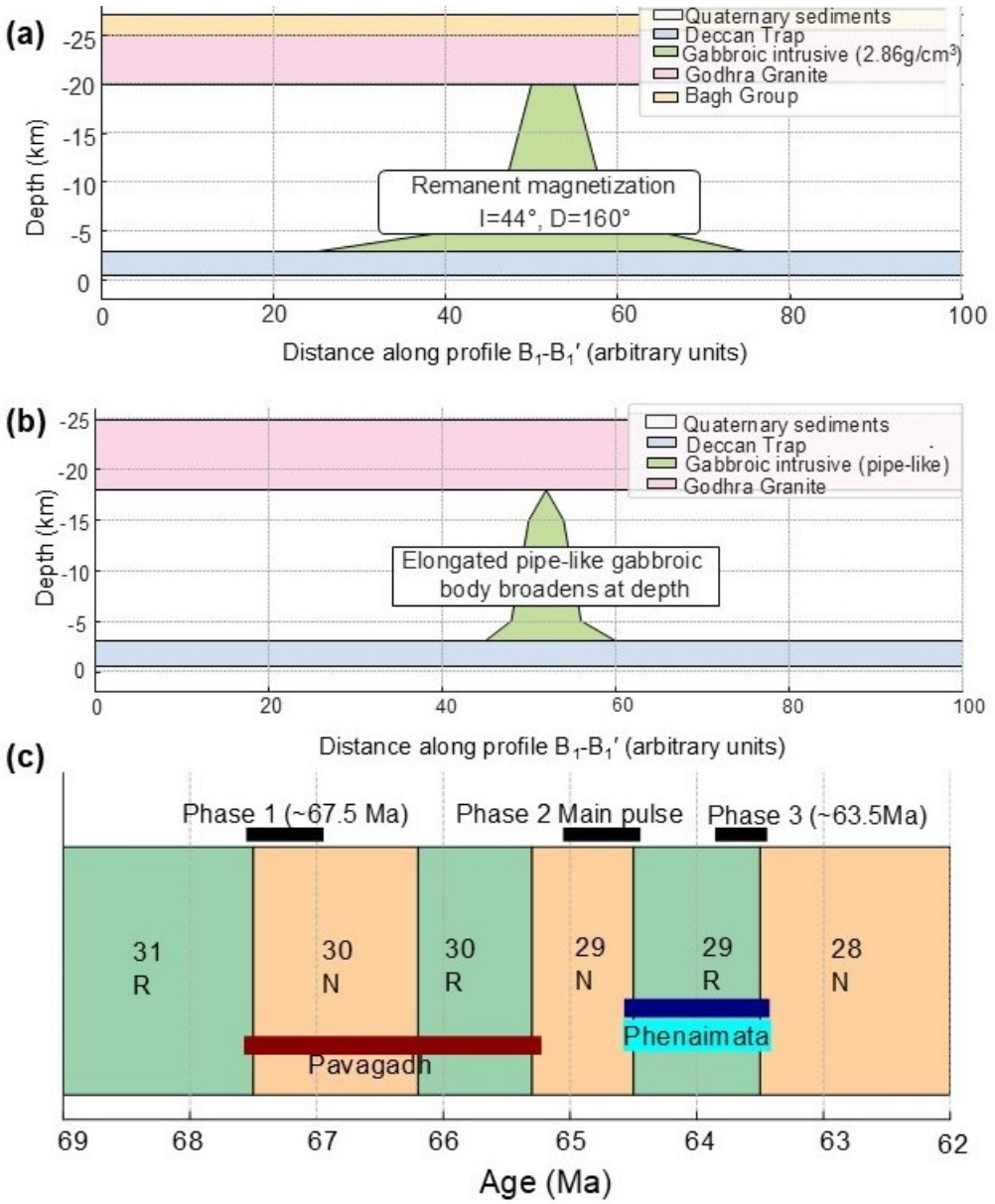

Figure 10. (**a**) 21/2-D joint gravity–magnetic model along profile B–B′ (Phenai Mata Igneous Complex). (**b**) $21/2-$D model along profile B1–B1′ (Phenai Mata Igneous Complex), (**c**) Deccan magnetostratigraphy and emplacement of Pavagadh and Phenai Mata intrusives.

5.4. Geochemical Evidence

Considering the vast diversity of the rocks occurring in the Chhota Udaipur alkaline-carbonatite sub-province, it is very arduous to compile and report all the varieties, because of which it is very important to define the context in which the geochemical data will be interpreted and select the data that can provide a significant and representative set of samples. The purpose of this compilation is to understand the space-time diversity among the magmatic rocks of CUACS. In this regard, the approach based on the concept of suites and series proposed by Gwalani et al. [4] is handy. The reason being, diversity in the intrusive rocks, that is lack of continuum of the rocks in a suite, leads to compositional gaps in the igneous rock suites. Such compositional gaps are the artefact of the combined processes of heat and water content of the magmas, especially that of the basaltic system [92]. Therefore, compositionally different-looking rocks could have a consanguinity among them. The concept of rock series is much older, having its roots in the initial experimental work of Prof. N. L. Bowen [93–97].

The dataset used for the present study comprises three series of rocks, namely, tholeiitic (gabbro and basalt); calc-alkaline or transitional (lamprophyre and picrobasalt), and alkaline (carbonatite and alkaline rocks such as nephelinite, phonolite, and ijolite). A total of 73 sample analyses were considered for the present study, out of which 19 gabbro and basalt samples represent tholeiitic series, 29 lamprophyre and picrobasalt samples represent transitional series, and 25 alkaline rocks including carbon-

atites represent alkaline series. In the above analyses, 12 lamprophyre analyses were taken from Randive et al. [48] and 25 alkaline rocks and carbonatite analyses were taken from Gwalani et al. [4]; rest of the data is taken from Randive [98]. Major elements were determined from fused pellets that were prepared by filling boric acid in Aluminum caps and about 2 g of finely powdered samples were sprinkled on the top of boric acid and pressed at 60 Pa. These fused pellets were analyzed on XRF Phillips MagiXPRO PW 2440, and the trace element and REE analysis was carried out using PerkinElmer Sciex ELAN DRC II system at the National Geophysical Research Institute (N.G.R.I.), Hyderabad following the standard operating procedure given in Randive et al [48] and the references therein.

The REEs are reliable indicators of source characterization and metasomatic processes [50, 99]. The combined scatter of all three series of rocks of CUACS brings forth a clear discrimination between the three series of rocks; whereas the tholeiitic rocks show less fractionated, and to some extent, flat pattern; the alkaline rocks show a highly fractionated pattern. The transitional series of rocks also shows a fractionated pattern but occupies space between the tholeiitic and alkaline series of rocks (Figure 11).

Some of the previous authors have mentioned MORB-like [82] and arc-like signatures in the CUACS rocks and the DLIP. To test these hypotheses, the trace-elements data of three series of rocks of the CUACS have been plotted using normalization from some of the crust and mantle reservoirs, namely, (a) primitive mantle (PM), (b) Normal MORB (N-MORB, (c) Enriched MORB (E-MORB), and Oceanic Island Basalt (OIB). If the CUACS data matches with, i.e., forms a flat pattern on this spider diagram with any of these reservoirs, then that will be the probable source of the CUACS magmas. The results of normalized plots are given in Figure 12.

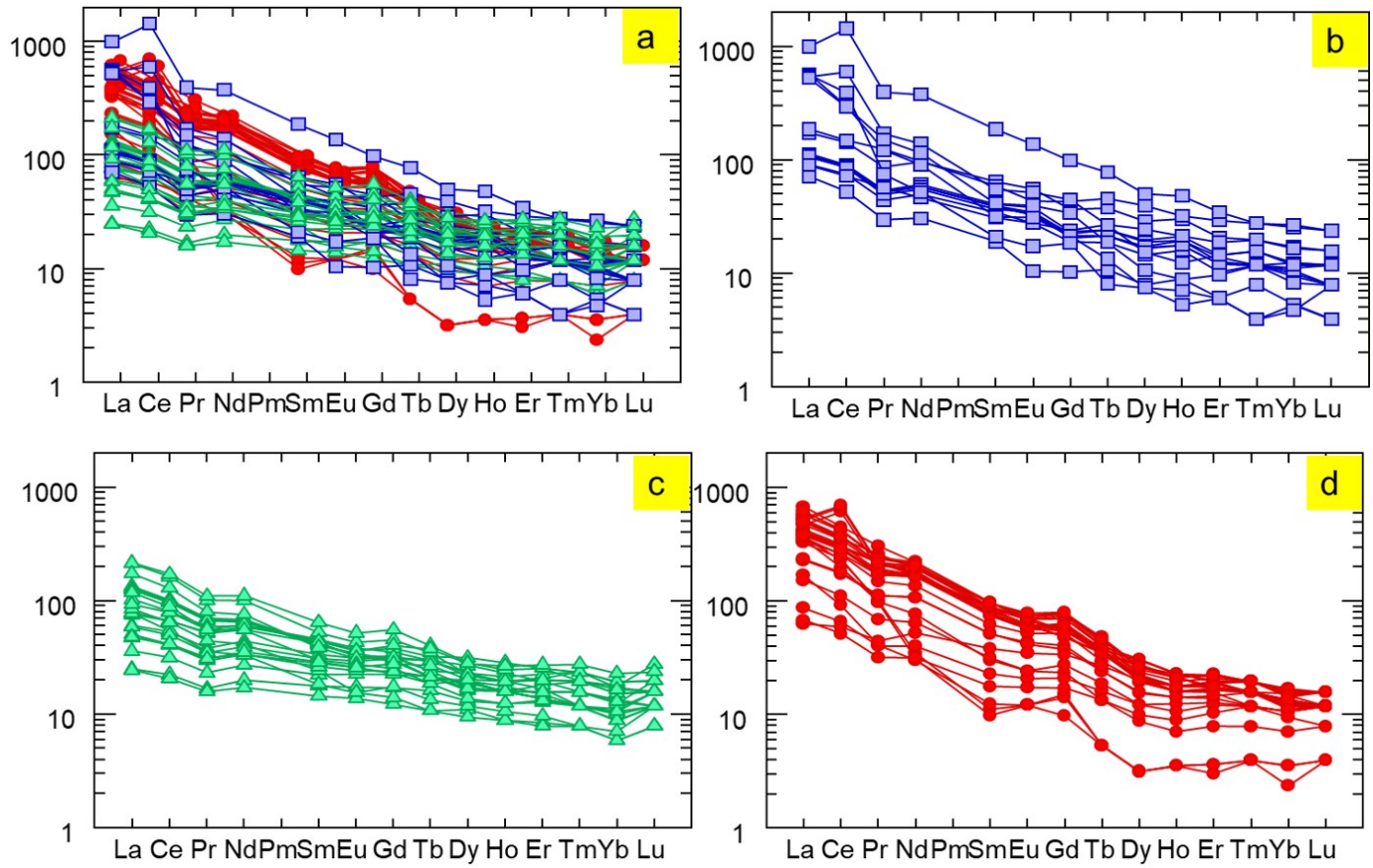

Figure 11. The rare earth elements spidergram showing chondrite normalized plots for alkaline (blue squares), calc-alkaline or transitional (red circles), and tholeiitic series (green triangles). Combined (**a**) as well as separate (**b**–**d**) plots for comparison show that alkaline rocks are more enriched compared to tholeiitic rocks, whereas the calc-alkaline rocks occur transitional between these two.

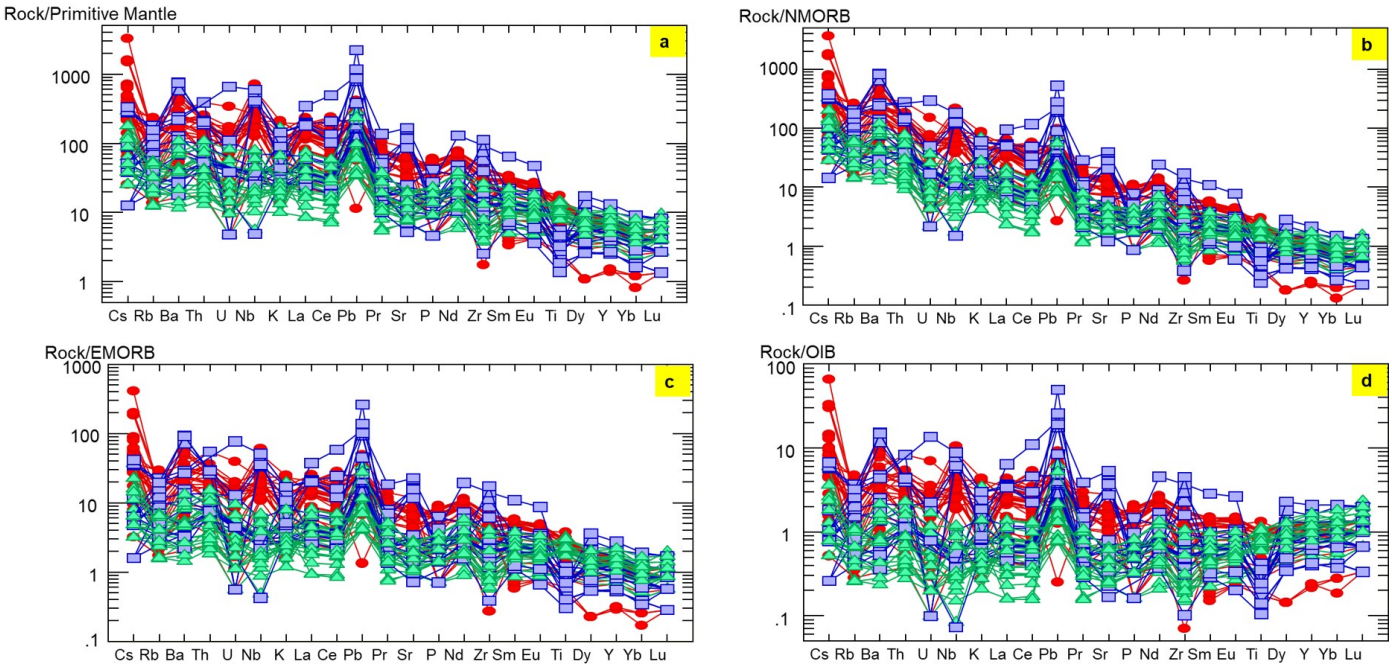

Figure 12. The trace elements spider diagram showing normalization of CUACS data with different reservoirs, namely, (**a**) Primitive Mantle, (**b**) N-MORB, (**c**) E-MORB, and (**d**) OIB. In these diagrams, the most prominent feature is the presence of high positive spikes for Pb, which unequivocally indicate the addition of crustal lead from the continental crustal or from the pelagic sediments. The NMORB normalized values show a highly fractionated pattern (**b**), whereas primitive mantle (**a**) and EMORB (**c**) normalized values show relatively less enrichment. The OIB normalized values are horizontal (flat), indicating consistency of values except Pb, which further confirms that the CUACS magmas, similar to the rest of the DLIP magmas, are inherited from the OIB-type mantle source. As compared to this, other sources, such as primitive mantle, NMORB, and EMORB, have distinct source characteristics. On the basis of these data, involvement of any other mantle source is negated. However, crustal contamination is clearly brought out.

In this figure, the N-MORB shows a highly fractionated pattern, which is due to a depleted-enriched contrast, which means that the CUACS rocks have no source inheritance from the depleted mantle component (N-MORB). The PM normalized as well as the E-MORB normalized (all normalization values are taken from Sun and McDonough [100]) diagrams also show fractionated patterns. Although they are not as much fractionated as N-MORB, apparently due to their enriched source (as in the Primitive Mantle) or subsequent enrichment (as in E-MORB), it is difficult to believe that they are the direct sources for the CUACS magmas. The OIB normalized patterns are, however, flat and horizontal, albeit with ruggedness in the spikes. Such a pattern indicates the source inheritance. Therefore, it is concluded here that the CUACS rocks were derived from the OIB-type enriched mantle source, and therefore, the possibility of involvement of multiple sources is not tenable. This also indicates that the CUACS rocks have formed in the same environment and therefore, they are related to one another on the basis of their source characteristics.

On the basis of trace elements geochemistry, from different discrimination diagrams and trace element ratios [101–105], a preliminary tectonic setting and petrogenetic history have been suggested. The major magma sources for different series of rocks can be reaffirmed from the discrimination diagrams (Figure 13a–e). The composition of the tholeiitic series of rocks of CUACS predominantly plots in the OIB field (Figure 13a,b). The MORB-OIB array produced by the OIB source is more enriched in comparison to MORB sources, as shown by their high Ta/Yb and Th/Yb ratios (Figure 13a,b). The Th/Yb ratios that plot above this MORB-OIB array are increased by crustal input, either via magma-crust interactions or by recycling of crust into magma sources. On the Ta/Yb versus Th/Yb diagram, the majority of data (tholeiitic and some calc-alkaline series of rocks) fall within an OIB field and move out of the main mantle array of basalts formed within the non-subduction setting. However, this is due to a relative increase in Ta and Th due to metasomatic effects, thereby reiterating that the inheritance of the CUACS magma is akin to a single source, i.e., OIB.

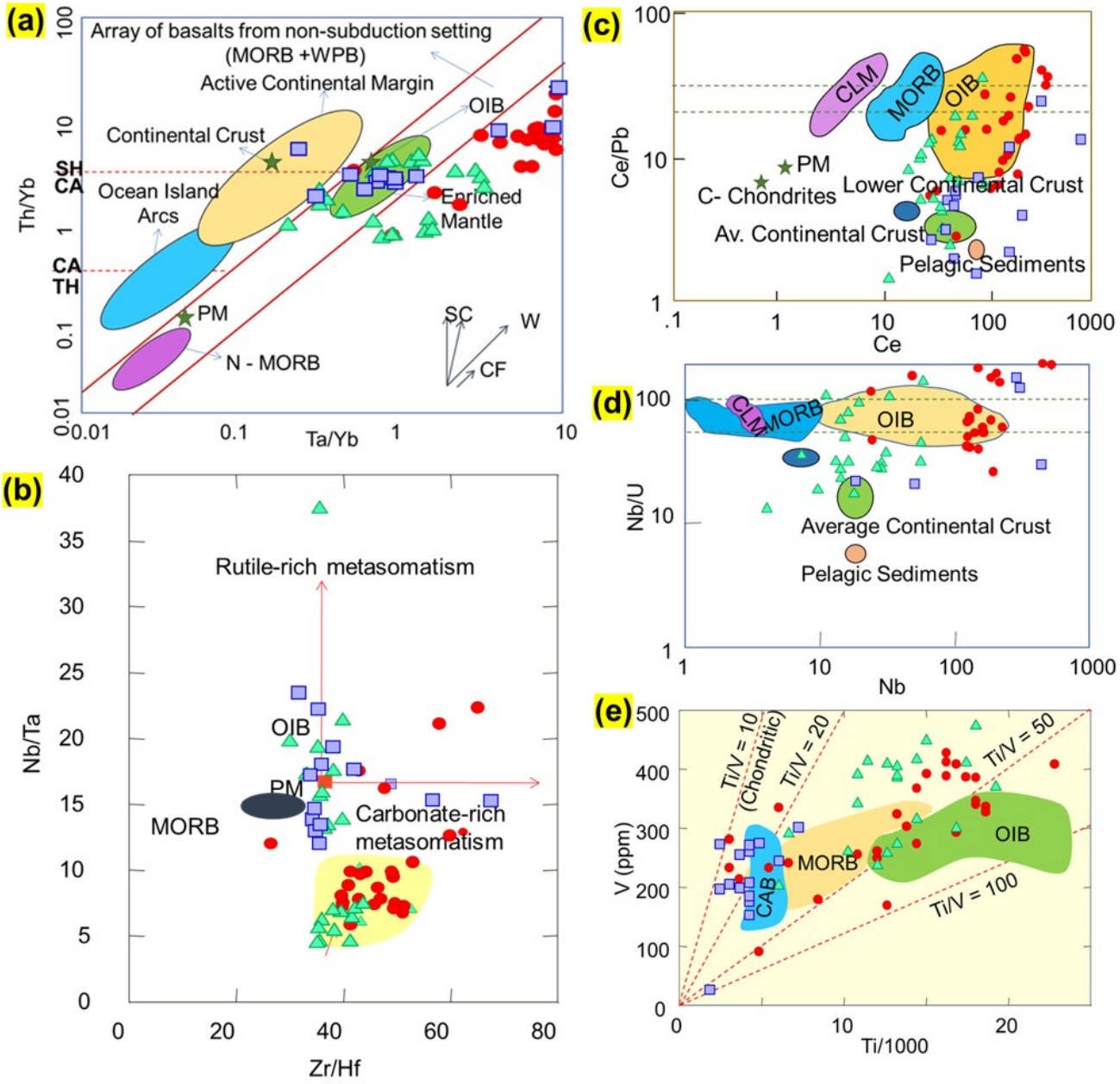

Figure 13. (**a**,**b**) The Ta/Yb vs Th/Yb discrimination diagram, showing that the majority of data falling within OIB (and enriched mantle) field and also lean towards the field of the continental crust. However, majority of data (notably, calc-alkaline and some alkaline series rocks) fall out of the mantle array, which is probably due to increase in Ta by metasomatism. (**b**) This is further observed in the Zr/Hf vs Nb/Ta plot, in which majority of tholeiitic and calc-alkaline rocks fall in a separate field, which is probably due to increase in Ta by metasomatic enrichment of the mantle. (**c**) The Ce/Pb vs Ce and (**d**) Nb/U vs Nb variation diagrams showing fields for CUACS rocks. Various crust and mantle components are plotted in comparison, namely, CLM—Continental Lithospheric mantle, MORB—Mid Oceanic Ridge Basalt, OIB—Oceanic Island Basalt, C-Chondrite—Carbonaceous Chondrites, and PM—Primitive Mantle. The data for all three series plot overwhelmingly in the OIB field and show a continuum with the crustal components in both diagrams. This confirms that the CUACS rocks are inherited from the OIB source and shows significant crustal contamination. (**e**) The Ti/V discrimination diagram. Symbols as per Figure, abbreviations: UCC—Upper Continental Crust, LCC—Lower Continental Crust, CAB—Calc-alkaline basalt, MORB—Mid Oceanic Ridge basalt, and OIB—Oceanic Island basalt. It is important to note that the expected value for Ti is 50 to 100 times greater than V. It is possible that there is reasonable interference in the signals of Ti and V; therefore, a possibility of matrix effect cannot be ruled out. Nonetheless, data show affinity towards the OIB source.

Similarly, other geochemical proxies such as Ce/Pb and Nb/U ratios are also used to evaluate the role of continental crust and pelagic sediments during their genesis [101, 102]. The CUACS rocks have a moderate to high Ce/Pb ratio, higher Nb/U and are plotted in the field of OIB and lower and upper continental crust. Some of these are plotted in the pelagic sediments field indicating crustal or pelagic sediments contamination (Figure 13c,d). However, the Nb versus Nb/U diagram shows that the majority of data points plot within the OIB field leaning towards the continental crust. This is also in confirmation with earlier view that the DLIP and CUACS magmas were derived from the OIB sources modified by crustal contamination [22].

Another discrimination diagram, Ti versus V [104], shows much scatter of data points occupying all three tectonic fields (Figure 13e). Therefore, on the whole, we didn't find any convincing evidence of the presence of MORB, IAT, PM, or HIMU-type mantle reservoirs. So far, the most convincing among all is the OIB-type source with smaller inputs from the continental crust and pelagic sediments. The same source is envisaged for all the intrusive rocks of the CUACS.

The εNd values of CUACS lamprophyres range from -2.5 to -7, and in the εNd(i) versus $^{87}Sr/^{86}Sr$(i) diagram (Figure 14), the CUACS lamprophyre samples are plotted in the domain of OIB-MORB mantle array with enriched mantle trend showing similarity to mantle characteristics like other Deccan lamprophyres. Moreover, the εNd(i) versus $^{87}Sr/^{86}Sr$(i) diagram (Figure 14) indicates that the samples plot within a mantle array near the Bulk Silicate Earth (BSE) axis. Most of the field area is enclosed by OIB (fields here are refereed from Tappe et al. [106] and references therein); however, one sample (KR/199) plots away towards a higher $^{87}Sr/^{86}Sr$(i) ratio. Since the lamprophyre and picrobasalt form the calc-alkaline or transitional series of rocks from the present study area that occur in the enriched mantle field, this further supports a single mantle source for the CUACS rocks.

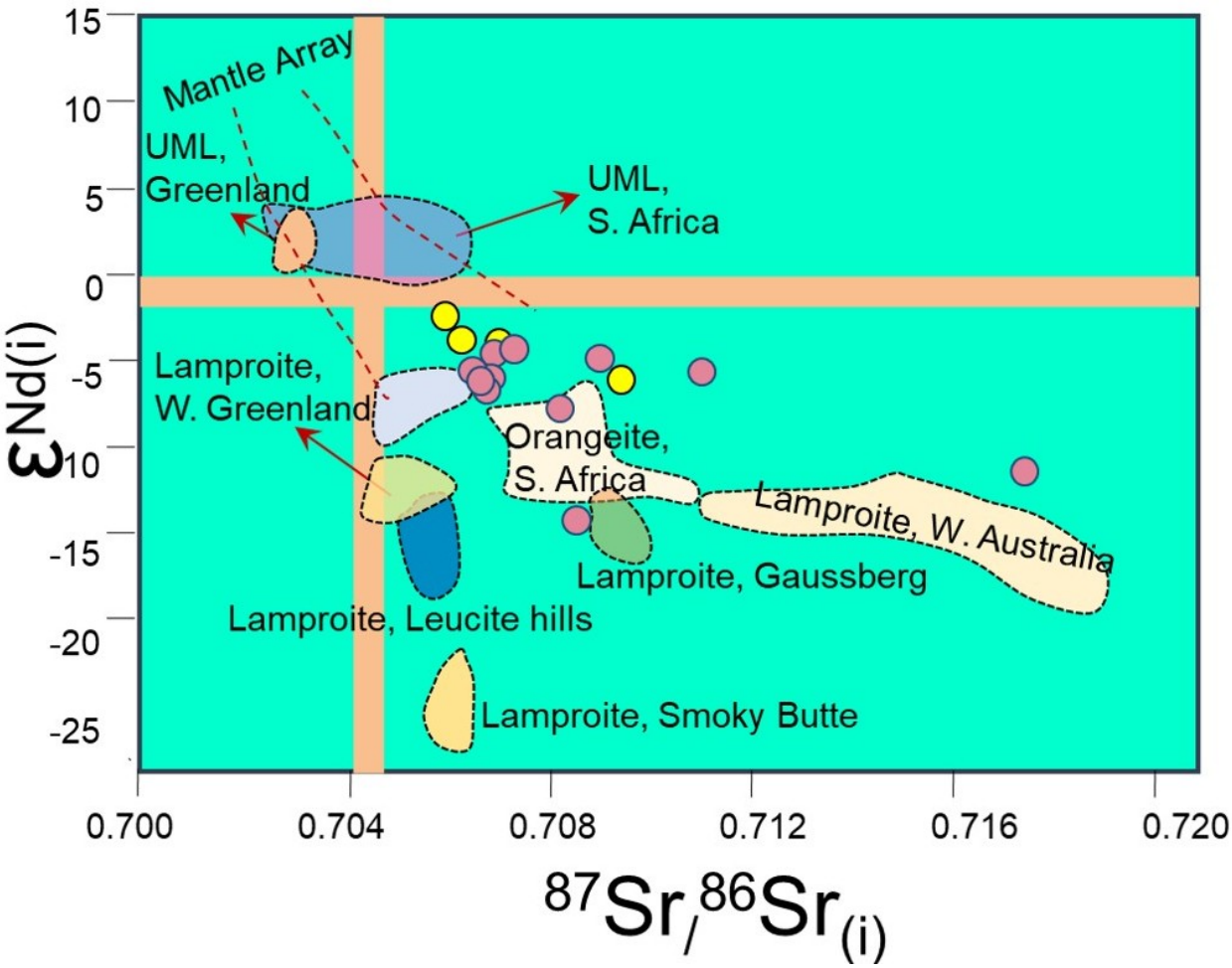

Figure 14. The $^{87}Sr/^{86}Sr$(i) vs εNd diagram plotting sample data from CUACS (i) Dungargaum lamprophyre. Most of the data points plot within the mantle array inside the enriched quadrant, except for those that show evolved nature. For comparison data fields of worldwide occurrences of similar rocks (UML, lamproites and orangeites) are also plotted. The $^{87}Sr/^{86}Sr$(i) vs εNd(i) plot showing scatter of data points for Dungargum lamprophyres. The data points plot within the mantle array inside the enriched quadrant. For comparison, data fields of worldwide occurrences of similar rocks (UML, lamproites, and orangeites) are also plotted.

5.5. Geochronological Evidence

Several recent studies have meticulously reviewed radiometric age data using high reliability and precision standards, leading to a reevaluation of the temporal framework of the DLIP. Studies are mainly based on high-precision U–Pb and ^{40}Ar/ ^{39}Ar geochronology. It indicates that the major phase of Deccan magmatism was short-lived and happened close to the Cretaceous–Paleogene boundary. Most of the eruptive volumes were emplaced over a short time span, in less than a million years [10, 11]. These evaluations on a province-wide scale give us a strong basis for reconsidering the geochronological characteristics of individual sub-provinces, including the Chhota Udaipur Alkaline–Carbonatite Sub-province. In this context, Baksi [10] critically reviewed Deccan age measurements again and showed that a lot of the apparent age variation is due to analytical uncertainties, alteration effects, and improper sample selection, and not because of prolonged or episodic magmatism. So, the geochronological data from the Chhota Udaipur Alkaline–Carbonatite Sub-province needs to be reviewed closely, as this area has yielded some of the most different age estimates in the Deccan province. Various dates available for the DLIP range from 80 Ma [107] to 37 Ma [108]. Based on these data, some authors postulated long-term episodic magmatism in the DLIP [81, 109, 110], whereas others, notably Baksi [10], debated that most of the earlier dates are either incorrect or based on flawed methods. A review of available age data of the Deccan LIP, especially in the context of the Chhota Udaipur area, is given below.

5.5.1. Age of the Deccan Traps

Earlier dates of the Deccan Traps indicate long-term (∼80 Ma) magmatism [107]. Recent studies by Kale et al. [40] proposed the protracted history of Deccan magmatism, which spans about 7 Ma. However, Baksi [10] has argued against this and previous research work that favoured an episodic magmatism within the DLIP. He founded his arguments on his reassessment of the available Ar^{40}/Ar^{39} ages for the Deccan trap lava flows from various stratigraphic units and/or their equivalents in the DLIP. He used the alteration index (AI) as the primary barrier to filter the age data using the technique discussed elaborately in Baksi [111, 112]. Secondly, the validity of plateau ages based on thermally equilibrated steps, whether they represent true crystallization ages, was critically examined. Baksi [10] concluded that many of the previously reported age data from different stratigraphic units of the DLIP do not qualify to this strict scrutiny based on the above two parameters. Thirdly, he also compared the ^{40}Ar/^{39}Ar whole rock ages and those of plagioclase separates with the U–Pb–Zr ages. These comparisons have yielded statistically significant dates for different stratigraphic units of the DLIP. Based on this, he rejected previously published ages, both upper and lower than the age bracket of about 66.3 to 66.5 Ma, which is less than 1 Ma. This feature of DLIP is similar to other continental flood basaltic provinces of the world, namely the Siberian Traps, the Parana-Etendeka, and the Columbia River basalt to have been erupted within a span of less than 1 Ma (e.g., Jiang et al. [11]; Kasbohm et al. [113]).

The age bracket given above confines to the main pulse of the Deccan magmatism reported as Composite Western Ghats Section (CWGS) [10]. This brief period of volcanic activity is also valid for the Mandla lobe, the Malwa plateau, the Rajahmundry traps, and some of the felsic and alkaline rocks in the Deccan Province, and possibly includes the tholeiitic rocks of the Phenai Mata area of the Chhota Udaipur Sub-province.

5.5.2. Age of the CUACS

Various authors have dated the rocks of CUACS; the data already available in the literature are considered and presented here to describe the space-time relationship of magmatic pulses (Figure 15). The earliest attempts included the dating of pyroxenes from nephelinite using the K/Ar method by Deans et al. [114], which yielded an age of 37.5 ± 2.5 Ma, and potash feldspar from the potassic fenites of Amba Dongar by Deans et al. [114], which yielded an age of 61 ± 2 Ma and 76 ± 2 Ma by the K–Ar method. Later, Veena et al. [115] dated carbonatite from the Siriwasan area that yielded an age of 71 ± 3 Ma using the Rb/Sr method and 72 ± 2 Ma using the Pb/Pb method. Similarly, ^{40}Ar/^{39}Ar geochronological analysis of biotite from Phenai Mata gabbro produced an age of 64.96 ± 0.11 Ma [19]. Viladkar and Gruau [116] and Petibon [117] in Viladkar [47] used phlogopite from a phlogopite-bearing fenite and obtained an age of 41.7 ± 3.2 Ma. A ^{40}Ar/^{39}Ar geochronological analysis of phlogopite from carbonatite and whole-rock nephelinite and tinguaite yielded an age of 65.0 ± 0.3 Ma [118, 119], whereas a phonolite from an alkaline plug dated by Ray et al. [120] produced an age of 65.2 ± 0.7 Ma using the Ar/Ar technique. Ray et al. [120] also dated basalt exposed inside the ring dyke of Amba Dongar and obtained an age of 68.5 ± 0.9 Ma. Similarly, Parisio et al. [121] dated 3 different samples of biotite and one amphibole from gabbroic rocks of Phenai Mata using the Ar/Ar method that yielded ages of 66.24 ± 0.37, 66.47 ± 0.34, 66.37 ± 0.31, and 66.60 ± 0.35 Ma, respectively. They also dated biotite in a lamprophyre dyke that yielded an age of 65.25 ± 0.29 Ma. Furthermore, the carbonatites of Siriwasan sill, dated by Viladkar and Gittins [122] using Rb/Sr, gave an age of 65.25 ± 0.29 Ma. Fosu et al. [123] and Chandra et al. [124] dated two apatite samples from the carbonatites and one from nephelinite using the Ar/Ar technique; a combined dataset gave an age of 65.4 ± 2.5 Ma. Basu et al. [125] using the U/Pb method dated gabbro from Phenai Mata yielding an age of 66.17 to 66.00 Ma. Table 1 compiles and summarizes the available ages of various rocks occurring in the Chhota Udaipur Sub-province.

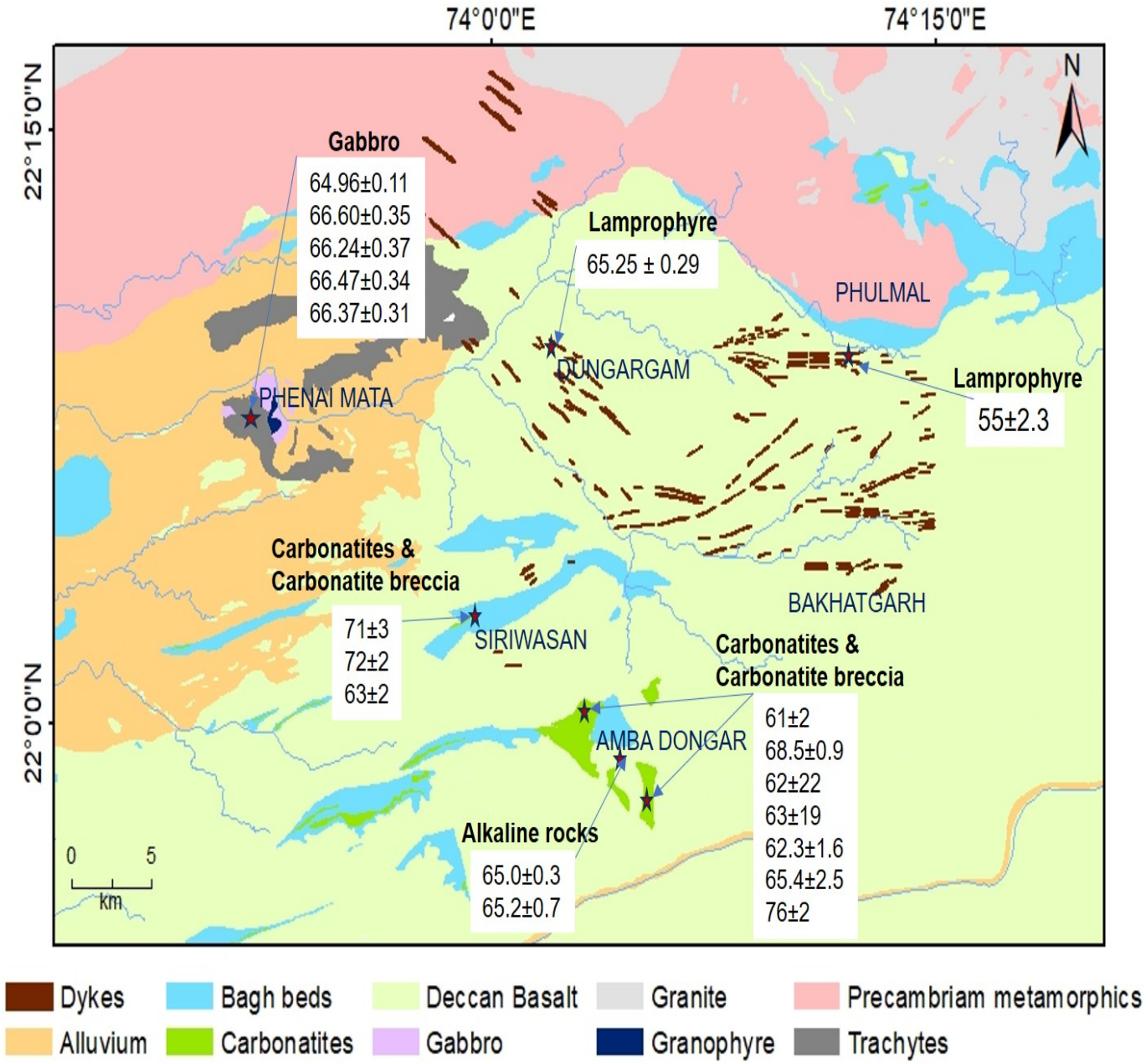

Figure 15. Map of Chhota Udaipur alkaline-carbonatite subprovince with the approximate location of the intrusive and alkaline bodies (red stars). The numbers in the boxes are the available ages (in Ma) of various rocks occurring in the Chhota Udaipur sub-province (the references for the ages given in Table 1).

Table 1. Sector-wise available ages of various rocks of CUACS.

Sector	Intrusives	Age	Dating Method	Reference
Amba Dongar	Alkaline rocks	37.5 ± 2.5 Ma (using pyroxenes from nephelinite)	Ar/Ar	[108]
	Carbonatites and carbonatite breccia	61 ± 2 Ma and 76 ± 2 Ma (using K-feldspar from potassic fenites)	K/Ar	[114]
	Carbonatites and carbonatite breccia	41.7 ± 3.2 Ma (using phlogopite from phlogopite-bearing fenite)	Rb/Sr	[116–118]
	Alkaline rocks	65.0 ± 0.3 Ma (Phlogopite from carbonatite and whole-rock nephelinite and tinguaite)	Ar/Ar	[118, 119]
	Alkaline rocks	65.2 ± 0.7 Ma (phonolite from an alkaline plug)	Ar/Ar	[120]
	Carbonatites and carbonatite breccia	68.5 ± 0.9 (basalt exposed inside the ring dyke)	Ar/Ar	[120]
	Carbonatites and carbonatite breccia	62 ± 22 and 63 ± 19 Ma (apatite from the carbonatites) 62.3 ± 1.6 Ma (apatite from nephelinite) 65.4 ± 2.5 Ma (three datasets combined on a U–Pb Tera–Wasserburg concordia plot)	U/Pb	[121, 122]
Phenai Mata	Layered gabbro-anorthosite–granophyre	64.96 ± 0.11 Ma (biotite from alkali olivine gabbro)	Ar/Ar	[121]
		66.60 ± 0.35 Ma (Amphibole)	Ar/Ar	[121]
		66.24 ± 0.37, 66.47 ± 0.34, 66.37 ± 0.31 (from 3 different samples of biotite from PM)	Ar/Ar	[121]
		66.17 to 66.00 Ma	U/Pb	[125]
Siriwasan-Dugdha	Carbonatites and carbonatite breccia	71 ± 3 Ma	Rb/Sr	[115]
	Carbonatites and carbonatite breccia	72 ± 2 Ma	Pb/Pb	[115, 122–124]
	Carbonatites and carbonatite breccia	63 ± 2 Ma	Rb/Sr	[122]
Panwad–Kawant	Lamprophyre-Picrobasalt dyke swarm	65.25 ± 0.29 Ma (from biotite in lamphrophyric dyke)	Ar/Ar	[121]
Bakhatgarh–Phulmal	Lamprophyre-Picrobasalt dyke swarm	55 ± 2.3 Ma (Lamprophyre)	Rb/Sr	[109]

6. Discussion

Interpretation of age relationships within the Chhota Udaipur Alkaline–Carbonatite Sub-province requires consideration of the temporal framework of the Deccan Large Igneous Province as a whole. Recent synthesis has shown that reliable constraints on the timing and duration of Deccan magmatism can only be obtained by focusing on the high-precision U–Pb and 40Ar/39Ar ages derived from well-preserved mineral phases. In this context, a comprehensive review of Phanerozoic Large Igneous Provinces is recently published by Jiang et al. [11], which provides an important reference for evaluating the Deccan geochronology.

Jiang et al. [11] further showed that, when only high-quality age data are considered, the Deccan magmatic event was a short span emplacement centered near the Cretaceous–Paleogene boundary. Much of the wide age range reported in earlier studies reflects analytical limitations, alteration of dated materials, or the use of less reliable methods, rather than genuine long-term or episodic magmatism. This conclusion is consistent with the present reassessment, which also argue for rapid emplacement of the Deccan flood basalts along with its derivative magmas emplaced in the form of several dykes, especially in the CUACS.

This wholistic perspective is essential for interpreting age data from the individual sub-provinces, as the variation in ages could be due to local challenges with sampling, post-emplacement alterations or analytical limitations rather than being actual different magmatic phases. In this context, the age data from the Chhota Udaipur Alkaline–Carbonatite Sub-province is reviewed to figure out their correlation with the overall timing of magmatism in the Deccan province.

Gwalani et al. [4] identified five suites of magmatic rocks in a chronological order from oldest to youngest as: (1) the tholeiitic suites comprising Deccan trap lava flows, (2) a layered gabbro-anorthosite-granophyre complex of Phenai Mata which intrude into the tholeiitic suite of basaltic lava flows, (3) the main alkaline intrusive suite which comprises of carbonatites and alkaline rocks, (4) a trachytic suite of dykes and plugs, and (5) the late basic-ultrabasic dykes and plugs which comprises of picritic basalt and dolerite. The above suites were classified based on ‘field relationship’ and ‘available age data’. However, more geochronological data have since been inundated in the literature. The chronology presented above remains unvalidated; on the contrary, we present below the absence of evidence to validate these chronological events.

(1) The tholeiitic suite comprising of the Deccan traps basaltic lava flows was considered to be the oldest among the rocks of CUACS. However, the relationship of the lava flows and intrusive igneous rocks (such as the alkaline-carbonatite suite of rocks) shows similar ages as that of the basaltic lava flows; high-precision $^{40}Ar/^{39}Ar$ ages obtained from the carbonatite complex of Mer-Mundwara (68.53 $\pm$ 0.16 Ma; [125]), Sarnu-Dandali (68.57 $\pm$ 0.08 Ma; [125]), and ages derived from K–Ar and $^{40}Ar/^{39}Ar$ dating from Amba Dongar (76 $\pm$ 2 Ma–61 $\pm$ 2 Ma; [114, 120, 123, 124]. These ages indicate that both basaltic lava flows and carbonatite-alkalic intrusive and extrusive rocks are akin to the same magmatic episode, e.g. Amba Dongar [126] and Girnar [127–130]. According to Krishnamurthy et al. [131], there is a Spatiotemporal sandwich of the tholeiitic and alkaline-intermediate-acidic magmatic pulses. According to these authors, the alkaline, intermediate, and acidic rocks occur sequentially during waxing and waning stages of the eruption of Deccan Traps basaltic lava flows. Therefore, alkaline and other rocks occurring within the DLIP are not temporally distinct and separable from the main pulse of the Deccan Traps basaltic magmatism.

(2) The Phenai Mata Igneous Complex (PMIC) has been dated precisely by $^{40}Ar/^{39}Ar$ geochronology to an age range of 64.96 $\pm$ 0.11 Ma–66.60 $\pm$ 0.35 Ma [20, 121]. Gwalani et al. [4] mentioned that the PMIC is ‘intrusive’ into a tholeiitic suite of basaltic lava flows. They also observed that this suite of rocks was intruded by a suite of alkaline rocks. It has been traditionally thought that the Phenai Mata layered igneous complex represents a differentiated suite of rocks starting from the layered gabbro to the granophyre end member [57, 58, 132]. However, Hari and Randive [73], Hari et al. [133], Randive et al. [134] presented a contradictory viewpoint in which these authors opined that the PMIC represents a bimodal suite of rocks that shows demonstrable mixing and mingling of magmas. Therefore, the hypothesis that the PMIC is intrusive into basaltic lava flows is no longer validated. The ages exhibited by the rocks of PMIC (gabbro and lamprophyre) show an age comparable to the carbonatite and alkaline rock of CUACS. Nevertheless, the ‘carbonatite breccia’ cutting across the granophyre-gabbro suite of PMIC is probably related to the late stage of magmatic/phreatomagmatic eruptions. Randive et al. [134] have reported a suite of REE-rich minerals such as synchysite, britholite, and REE-rich epidote, which they assigned to a late-stage hydrothermal imprint over the PMIC area. Thus, the status of layered gabbro and the associated rocks of PMIC remains unassigned due to similar ages between the layered tholeiitic gabbro-anorthosite-granophyre suite of PMIC and the main alkaline intrusive suite of Amba Dongar and Panvad-Kawant.

(3) However, the position of trachytic suit of rock remains unclear due to the paucity of any age data on these rocks. In fact, except for Gwalani [53] and Gwalani et al. [4], there is no literature available on these rocks. During our fieldwork, we found a large number of small trachyte dykes intruding within the Deccan Traps basaltic lava flows. Although it is difficult

to assign an age bracket to this rock, it is unlikely to deviate from the other intrusive rocks within the CUACS.

Similarly, not much age data is available from the Bakhatgarh–Phulmal sector; several dykes of picrobasalt and lamprophyre show continuity with those in the Panwad–Kawant sector. A majority of dykes occurring in this sector are of 'calcareosiliceous' composition. These are not true carbonatites, and probably not formed due to bonafied magmatic processes [5, 48, 50, 63]. Therefore, we do not find any reason to believe that these rocks are 'younger' to the main suite of alkaline–carbonatite magmatism.

The total available geochronological data (dates) are synthesized sector-wise in the following discussion to build a space-time relationship among the lithologies present in the CUACS. In the end, the validity of the dates is argued on the basis of the robustness of the technique that was used to obtain these dates.

The Amba Dongar rocks have received much attention from the beginning. The first date came from the mineral dating, including K–Ar analyses of pyroxenes from nephelinite (37.5 $\pm$ 2.5 Ma by Deans and Powell [108]) and K–Ar dating of potash feldspar from fenites (61 $\pm$ 2 Ma and 76 $\pm$ 2 by [114]). These two dates were almost unanimously believed to be erroneous [4]. Other dates of 61 $\pm$ 2 Ma and 76 $\pm$ 2 Ma were obtained using K–Ar dating. In most cases, including this, an argon loss and excess argon are two typical issues that may lead to inaccurate age determinations. High temperatures and alteration may liberate ^{40}Ar from rock/mineral lattices, which might deviate from the estimated K/Ar age. Therefore, the excess argon might make the computed K/Ar age older than the "actual" age of the dated sample [135]. In this case, both the dates are $\pm$5–10 Ma, deviated from the main magmatic pulse of Deccan basalt [10]. The alkaline rocks from the Amba Dongar sector were also dated by Ray and Pande [119], Ray et al. [118–120], by the Ar/Ar method. The dates obtained by these authors are very precise, i.e. 65.2 $\pm$ 0.7 Ma and 65.0 $\pm$ 0.3 Ma. These dates are closer to the main magmatic pulse, albeit on the lower side by $\leq$1 Ma. Baksi [90] does not seem to have attempted recalculation of plateau ages, which is likely to bring down these dates into the same bracket of ages, confirming the main pulse of Deccan trap basaltic magmatism. Ray et al. [120] also obtained an age of 68.5 $\pm$ 0.9 Ma for the basalt present inside the carbonatite ring dyke using Ar/Ar method. In this case, the age seems to be misleading; mainly for the fact that if the core basalt (the basaltic plug inside the ring dyke) is older to the carbonatite intrusion, then in all probability, it will be too altered to give an accurate age. Fosu et al. [123] and Chandra et al. [124] used fission track dating of apatite from carbonatite and nephelinite of Amba Dongar using the U/Pb method. These authors have produced four dates, of which apatite from carbonatite has yielded 62 $\pm$ 2.2 Ma and 63 $\pm$ 1.9 Ma; 62.3 $\pm$ 1.6 Ma for apatite from nephelinite; and the combined age of 65.4 $\pm$ 2.5 Ma using U/Pb Tera-Wasserburg Concordia plot. According to these authors, the later recalculated age of 65.4 $\pm$ 2.5 Ma is more likely to be a realistic age estimate for the Amba Dongar rocks. Despite different techniques used, it is apparent that the techniques have their inherent problems of measurements, assumptions, calculations, and extraneous problems such as alteration, which are major impediments to their accurate prediction. Such problems related to the Ar/Ar technique were discussed earlier by Baksi [90, 111, 112].

The 11 km long carbonatite sill of the Siriwasan-Dugdha sector [4, 136] is another major center of carbonatitic magma eruption in the CUACS. The available dates are from Veena et al. [115] and Viladkar and Gittins [122]. The former authors obtained 71 $\pm$ 3 Ma using Rb/Sr and 72 $\pm$ 2 Ma using Pb/Pb. Viladkar and Gittins [122] have also obtained the dates from Siriwasan using the Rb/Sr method, but they claimed their date of 63 $\pm$ 2 Ma is more precise than that of Veena et al. [115]. However, the dates of later authors also seem to be on the lower side. In every possibility, the chances of alteration, metasomatism, and mixing of crustal components and porous water within the sandstone in which these carbonatites have been intruded make the reliability of these dates questionable.

The Phenai Mata is one of the most precisely dated sectors of CUACS. Earlier dates have been given by Basu et al. [20], who obtained the date of 64.96 $\pm$ 0.1 Ma for the biotite separates using the Ar/Ar method. Baksi [90] questioned these dates. Basu et al. [125] recalculated the ages of Phenai Mata gabbro; this time using U/Pb geochronometry and obtained their dates of 66.17–66.00 Ma, which seems to be the most accurate dates available so far from the CUACS. This date is also coeval with the main pulse of Deccan basaltic magmatism in the Composite Western Ghats section (CWGS) of the DLIP [90]. Parisio et al [121] proposed Ar/Ar dates for amphibole and biotite gabbro of Phenai Mata to be around 66.60 $\pm$ 0.35 Ma, 66.24 $\pm$ 0.37 Ma, 66.47 $\pm$ 0.31 Ma. These ages are in good agreement with the U/Pb ages given by Basu et al [125].

Parisio et al. [121] have also dated biotite in a lamprophyre dyke in the Dungargum area by Ar/Ar method. They obtained an age of 65.25 $\pm$ 0.29 Ma for the biotite separates using Ar/Ar method. This age falls within a range of $\pm$ 1 Ma for CWGS ages of DLIP. It also indicates that the lamprophyres are younger in the sequence, which is also confirmed by their intrusive relationship elsewhere [137]. The Dungargum area is a part of the Panwad–Kawant sector [4]. Similarly, the lamprophyre dated from nearby areas of the Bakhatgarh–Phulmal sector dated by Sahu et al [110] gives a much younger age of 55 $\pm$ 2.3 Ma using Rb–Sr technique. In all probability, Parisio et al [121] and Randive et al [103] have dated similar dykes by using different techniques, of which the former age is more reliable.

To sum up, the ages obtained from the CUACS appear to be distinct in space (sector-wise) as well as time (age-wise/ temporal). The above discussion favors the most reliable ages across the sector based on the reasoning given in the Table 2.

Table 2. Reported ages across the sectors and their reliability.

Sr. no.	Sector	Obtained Ages	Accepted Ages	Discarded Ages	Remarks
1.	Amba Dongar	37.5 ± 2.5 Ma (using pyroxenes from nephelinite) [108]		37.5 ± 2.5 Ma	The alteration may be responsible for inaccurate age determination
		61 ± 2 Ma and 76 ± 2 Ma (using K-feldspar from potassic fenites [114])		61 ± 2 Ma and 76 ± 2 Ma	The K–Ar technique cannot be considered suitable for dating younger rocks. Here, a deviation of ±5–10 Ma from the main magmatic pulse
		41.7 ± 3.2 Ma (using phlogopite from phlogopite-bearing fenite) [116, 117]		41.7 ± 3.2 Ma	Inaccurate age
		65.0 ± 0.3 Ma (Phlogopite from carbonatite and whole-rock nephelinite and tinguaite) [118, 119]	65.0 ± 0.3 Ma		The precise date, closest to the main magmatic pulse
		65.2 ± 0.7 Ma (phonolite from an alkaline plug) [120]	65.2 ± 0.7 Ma		The precise date, closest to the main magmatic pulse
		68.5 ± 0.9 Ma (basalt exposed inside the ring dyke) [120]		68.5 ± 0.9 Ma	The sample is most likely to be too altered
2.	Siriwasan-Dugdha	71 ± 3 Ma (Rb–Sr isochron age [115])		71 ± 3Ma	Alteration, metasomatism, and mixing of crustal components from the sandstone to which these carbonatites have been intruded make the dates less reliable.
		72 ± 2 Ma (whole-rock and mineral Rb–Sr) [115, 122–124]		72 ± 2 Ma	
		63 ± 2 Ma (K–Ar on phlogopite [122])		63 ± 2 Ma	Much on the lower side than the main magmatic pulse
3.	Phenai Mata	64.96 ± 0.11 Ma (biotite from alkali olivine gabbro) [20]		64.96 ± 0.11 Ma	On the lower side than the main magmatic pulse
		66.60 ± 0.35 Ma (Amphibole) [121]	66.60 ± 0.35 Ma		Dates are in good agreement (Reliable dates)
		66.24 ± 0.37, 66.47 ± 0.34, 66.37 ± 0.31 (from 3 different samples of biotite from PM) [121]	66.24 ± 0.37, 66.47 ± 0.34, 66.37 ± 0.31		
		66.17 to 66.00 Ma [125]	66.17 to 66.00 Ma		
4.	Panwad–Kawant	65.25 ± 0.29 Ma (from biotite in lamprophyre dyke) [121]	65.25 ± 0.29 Ma		Reliable age
5.	Bakhatgarh–Phulmal	55 ± 2.3Ma (Lamprophyre) [109]		55 ± 2.3Ma	Erroneous age

The most reliable age dates of the CUACS are confined to 66 $\pm$ 1 Ma, which is equivalent to the main pulse of Deccan basaltic magmatism (CWGS), and shows a very narrow age bracket and which is also a characteristic of the large igneous provinces (Baksi, [136] and references therein). It is therefore observed that there is no unambiguous and demonstrable episodic magmatism in the CUACS; on the contrary, there are demonstrable evidences that the geochronological data showing so-called magmatic pulses are flawed and subject to reinterpretation. Despite being spatially separated, the intrusive or extrusive rocks of the CUACS are coeval, and there is no episodic magmatism in the CUACS.

7. Concluding Remarks

The high-precision U–Pb and $^{40}Ar/^{39}Ar$ geochronology has firmly established that the Deccan Large Igneous Province formed during a geologically brief time interval close to the Cretaceous–Paleogene boundary. Within this well-constrained temporal framework, the present study was aimed to characterize the poorly understood Chhota Udaipur Alkaline-Carbonatite Sub-Province (CUACS) and to evaluate its spatial and temporal relationship with the Deccan magmatic event. Field relationships, structural patterns, petrographic characteristics, and geochemical signatures across the CUACS reveal no compelling evidence for temporally distinct intrusive episodes. Instead, the diverse alkaline, transitional, and tholeiitic rock suites show coherence in source characteristics and emplacement relationships. When critically assessed, reported older ($>$68 Ma) and younger ($\sim$61–64 Ma) ages appear inconsistent and are best explained by analytical uncertainties or altered samples rather than by prolonged or episodic magmatism. Overall, the CUACS magmatism is interpreted to be broadly coeval with the principal Deccan eruptive phase at $\sim$66 Ma. These findings reinforce the view that the Deccan magmatic system, including its alkaline-carbonatite components, represents a short-lived but compositionally diverse magmatic episode rather than a temporally extended or episodic magmatism.

Author Contributions

Conceptualization K.R.; methodology, S.J. and K.R.; investigation and fieldwork, K.R.; formal analysis, S.J. and K.R.; writing—original draft preparation, S.J.; writing—review and editing, K.R.; supervision, K.R. All authors have read and approved the final version of the manuscript.

Funding

Funding received from Anusandhan National Research Foundation (ANRF), New Delhi, through research project No EMR/2017/003099.

Institutional Review Board Statement

Not applicable.

Informed Consent Statement

Not applicable.

Data Availability Statement

The data presented in this study are available from the corresponding author upon reasonable request.

Acknowledgements

We acknowledge the generous funding received from Anusandhan National Research Foundation (ANRF), New Delhi, through research project No EMR/2017/003099. We sincerely thank H. Bilal and an anonymous reviewer for thoroughly reviewing our manuscript and offering useful comments and criticism for improving the original manuscript. Shakthi Sarvanan, who invited KRR to write for the inaugural issue of the journal, and to M. Santosh, for supporting us at all stages. We also acknowledge the help and support given by Tejashree and Sneha during fieldwork, and by Prateek and Kritika during the final stages of the manuscript preparation. This work is a contribution of the Critical Minerals Research Centre (CMRC), RTM Nagpur University.

Conflicts of Interest

The authors declare that they have no known competing financial interests or personal relationships that could have appeared to influence the work reported in this paper.

Use of AI and AI-Assisted Technologies

During the preparation of this work, the authors did not use artificial intelligence (AI) or AI-assisted technologies.

References

1. Subba Rao, S.S. Alkaline Rocks of the Deccan Traps. *Bull. Volcanol.* **1971**, *35*, 998–1011. https://doi.org/10.1007/BF02596861
2. Bose, M.K. Alkaline Volcanism in the Deccan Volcanic Province. *J. Geol. Soc. India* **1980**, *21*, 317–329.
3. Sethna, S.F. Petrology and geochemistry of the acid, intermediate and alkaline rocks associated with the Deccan basalt in Gujarat and Maharashtra. *Mem. Geol. Soc. India* **1989**, *15*, 47–61.
4. Sethna, S.F.; Borges, S.M. Petrology of the Carbonatites and Associated Alkaline Rocks of Siriwasan, Cahota Udaipur *J. Geol. Soc. India* **1981**, *22*, 417–425.
5. Randive, K.R. Intrusive dykes of Chhaktala, Jhabua district, Madhya Pradesh: Field relations, petrography and petrochemical characteristics with reference to their PGE concentration. *J. Econ. Geol. Georesour. Manag.* **2005**, *2*, 117–137.
6. Lehmann, B.; Burgess, R.; Frei, D.; et al. Diamondiferous kimberlites in Central India synchronous with Deccan flood basalts. *Earth Planet. Sci. Lett.* **2010**, *290*, 142–149. https://doi.org/10.1016/j.epsl.2009.12.014
7. Renne, P.R.; Sprain, C.J.; Richards, M.A.; et al. State shift in Deccan volcanism at the cretaceous–paleogene boundary, possibly induced by impact. *Science* **2015**, *350*, 76–78. https://doi.org/10.1126/science.aac7549
8. Schoene, B.; Eddy, M.P.; Samperton, K.M.; et al. U-Pb constraints on pulsed eruption of the Deccan Traps across the end-Cretaceous mass extinction. *Science* **2019**, *363*, 862–866.

https://doi.org/10.1126/science.aau2422

9. Sprain, C.J.; Renne, P.R.; Vanderkluysen, L.; et al. The eruptive tempo of Deccan volcanism in relation to the Cretaceous-Paleogene boundary. *Science* **2019**, *363*, 866–870. https://doi.org/10.1126/science.aav1446
10. Baksi, A.K. Geochemistry and geochronology of the Rajmahal flood basalt province, Northeastern India: Genetic links to Kerguelen hotspot activity. *J. Earth Syst. Sci.* **2022**, *131*, 1–10. https://doi.org/10.1007/s12040-022-01855-8
11. Jiang, Y.; Ernst, R.E.; Peate, D.W.; et al. An appraisal of the ages of Phanerozoic large Igneous provinces. *Earth Sci. Rev.* **2023**, *237*, 104314. https://doi.org/10.1016/j.earscirev.2023.104314
12. Ernst, R.E.; Bell, K. Large Igneous provinces (LIPs) and carbonatites. *Miner. Petrol.* **2010**, *98*, 55–76. https://doi.org/10.1007/s00710-009-0074-1
13. Pande, K. Age and duration of the deccan traps, India: A review of radiometric and paleomagnetic constraints. *Proc. Indian Acad. Sci. Earth Planet. Sci.* **2002**, *111*, 115–123.
14. Chenet, A.L.; Quidelleur, X.; Fluteau, F.; et al. 40Ar/39Ar Dating of the main Deccan large Igneous province: Further evidence of KTB age and short duration. *Earth Planet. Sci. Lett.* **2007**, *263*, 1–15. https://doi.org/10.1016/j.epsl.2007.07.011
15. Hooper, P.R.; Widdowson, M.; Kelley, S.P.; et al. Tectonic setting and timing of the final Deccan flood basalt eruptions. *Geology* **2010**, *38*, 839–842. https://doi.org/10.1130/G31072.1
16. Valdiya, K.S. *The Making of India Geodynamic Evolution*; Macmillan Publishers: New York, NY, USA, 2010; p. 816.
17. Valdiya, K.S. Some burning questions remaining unanswered. *J. Geol. Soc. India* **2011**, *78*, 299–320. https://doi.org/10.1007/s12594-011-0097-1
18. Baksi, A.K. Geochronological studies on the whole-rock basalts, Deccan traps, India: Evolution of the timing of volcanism relative to the K-T boundary. *Earth Planet. Sci. Lett.* **1994**, *121*, 43–56. https://doi.org/0012-821X(94)90030-2
19. Baksi, A.K. The Deccan Trap – Cretaceous–Palaeogene Boundary connection: New 40Ar/39Ar Ages and critical assessment of existing argon data pertinent to this hypothesis. *J. Asian Earth Sci.* **2014**, *84*, 9–23. https://doi.org/10.1016/j.jseaes.2013.08.021
20. Basu, A.R.; Renne, P.R.; DasGupta, D.K.; et al. Early and late alkali Igneous pulses and a high-3He Mantle source for the Deccan flood basalts, India. *Science* **1993**, *261*, 902–906. https://doi.org/10.1126/science.261.5123.902
21. Sen G.; Hames, W.E.; Paul, D.K.; et al. Pre-Deccan and Deccan magmatism in Kutch, India: Implications of New 40Ar/39Ar ages of intrusions. *J. Geol. Soc. India* **2016**, *Special Publication No. 6*, 211–222. https://doi.org/10.17491/cgsi/2016/105422
22. Kumar, J.V.; Randive, K. Platinum group elements in lamprophyre, picrobasalt, gabbro and basalts of the Phenai Mata and nearby areas: Implications for Fe–Ni–Cu–PGE mineralization in the Deccan Large Igneous Province. In *Lamprophyres, Lamproites and Related Rocks: Tracers to Supercontinent Cycles and Metallogenesis*; Krmíček, L., Chalapathi Rao, N.V., Eds.; Geological Society: London, UK, 2022. https://doi.org/10.1144/SP513-2020-265
23. Coffin, M.F.; Eldholm, O. Large Igneous Provinces: Crustal structure, dimensions, and external consequences. *Rev. Geophys.* **1994**, *32*, 1–36. https://doi.org/10.1029/93RG02508
24. Courtillot, V.E.; Renne, P.R. On the ages of flood basalt events. *C. R. Geosci.* **2003**, *335*, 113–140. https://doi.org/10.1016/S1631-0713(03)00006-3
25. Neal, C.R.; Coffin, M.F.; Arndt, N.T.; et al. Investigating Large Igneous Province formation and associated Paleoenvironmental events: A white paper for scientific drilling. *Sci. Drill.* **2008**, *6*, 4–18. https://doi.org/10.04/iodp.sd.6.01.008
26. Ernst, R.E. *Large Igneous Provinces*; Cambridge University Press: Cambridge, UK, 2014; p. 666. https://doi.org/10.1017/CBO9781139025300
27. Mahoney, J.J. Deccan traps. In *Continental Flood Basalts*; Macdougall, J.D., Ed.; Kluwer Academic: Dordrecht, The Netherlands, 1988; pp. 151–194.
28. Jay, A.E.; Widdowson, M. Stratigraphy, structure and volcanology of the SE Deccan continental flood Basalt Province: Implications for eruption mechanisms. *J. Geol. Soc. Lond.* **2008**, *165*, 177–188. https://doi.org/10.1144/0016-76492006-062
29. Mahoney, J.J.; Duncan, R.A.; Khan, W.; et al. Cretaceous volcanic rocks of the South Tethyan Suture Zone, Pakistan: Implications for the reunion hotspot and the Deccan traps. *Earth Planet. Sci. Lett.* **2002**, *203*, 295–310. https://doi.org/10.1016/S0012-821X(02)00840-3
30. Collier, J.S.; Sansom, V.; Ishizuka, O.; et al. Age of Seychelles–India break-up. *Earth Planet. Sci. Lett.* **2008**, *272*, 264–277. https://doi.org/10.1016/j.epsl.2008.04.045
31. Mahoney, J.J.; Macdougall, J.D.; Lugmair, G.W. Kerguelen hotspot source for Rajmahal traps and Ninetyeast ridge? *Nature* **1983**, *303*, 385–389.
32. Watts, A.B.; Cox, K.G. The Deccan traps: An interpretation in terms of progressive lithospheric thinning beneath the Indian Continent. *Earth Planet. Sci. Lett.* **1989**, *93*, 85–97. https://doi.org/10.1016/0012-821X(89)90186-6
33. Sheth, H.C. From Deccan to Réunion: No trace of a mantle plume. In *Plates, Plumes and Paradigms*; Foulger, G.R., Natland, J.H., Presnall, D.C., et al., Eds.; Geological Society of America: Boulder, CO, USA, 2005; Volume 388, pp. 477–501. https://doi.org/10.1130/0-8137-2388-4.477
34. Hooper, P.R.; Widdowson, M.; Kelley, S. Tectonic setting and timing of the Deccan Traps. *Geology* **2010**, *38*, 839–842. https://doi.org/10.1130/g31072.1
35. Baksi, A.K. Timing and duration of volcanism in the Columbia River Basalt Group: A review of existing radiometric data and new constraints on the age of the Steens through Wanapum Basalt extrusion. *Geol. Soc. Am. Spec. Pap.* **2013**, *497*, 67–85. https://doi.org/10.1130/2013.2497(03)
36. Kasbohm, J.; Schoene, B. Rapid eruption of the Columbia River flood basalt and correlation with the mid-miocene climate optimum. *Sci. Adv.* **2018**, *4*, eaat8223. https://doi.org/10.1126/sciadv.aat8223
37. Renne, P.; Ernesto, M.; Pacca, I.; et al. The age of Parana flood volcanism, rifting of Gondwanaland, and the Jurassic-cretaceous boundary. *Science* **1992**, *258*, 975–979. https://doi.org/10.1126/science.258.5084.975
38. Baksi, A.K. Paraná flood basalt volcanism primarily limited to ~ 1 Myr beginning at 135 Ma: New 40Ar/39Ar ages for rocks from Rio Grande do Sul, and critical evaluation of published radiometric data. *J. Volcanol. Geotherm. Res.* **2018**, *355*, 66–77. https://doi.org/10.1016/j.jvolgeores.2017.02.016
39. Renne, P.R.; Basu, A.R. Rapid eruption of the Siberian traps flood basalts at the permo-triassic boundary. *Science* **1991**, *253*, 176–179. https://doi.org/10.1126/science.253.5016.176
40. Kale, V.; Achalla, G.; Shandilya, P.; et al. Stratigraphy and correlations in Deccan Volcanic Province, India: Quo vadis? *GSA Bull.* **2019**, *132*, 588–607. https://doi.org/10.1130/B35018.1
41. Baksi, A.K. Corrigendum to "The Deccan Traps – Cretaceous–Paleogene boundary connection; new 40Ar/39Ar ages and critical assessment of existing argon data pertinent to this hypothesis". [J. Asian Earth Sci. 84 (2014) 9–23]. *J. Asian Earth Sci.* **2016**, *120*, 193. https://doi.org/10.1016/j.jseaes.2016.01.020
42. Schoene, B.; Eddy, M.P.; Samperton, K.M.; et al. U–Pb geochronology of the Deccan traps and relation to the end-cretaceous mass extinction. *Science* **2015**, *347*, 182–184. https://doi.org/10.1126/science.aaa0118
43. Schoene, B.; Eddy, M.; Samperton, K.; et al. U-Pb constraints on pulsed eruption of the Deccan Traps across the end-Cretaceous mass extinction. *Science* **2019**, *363*, 862–866. https://doi.org/10.1126/science.aau2422

44. Sprain, C.J.; Renne, P.R.; Vanderkluysen, L.; et al. The eruptive tempo of Deccan volcanism in relation to the Cretaceous-Paleogene boundary. *Science* **2019**, *363*, 866–870. https://doi.org/10.1126/science.aav1446
45. Eddy, M.P.; Schoene B.; Samperton K.M; et al. U-Pb zircon age constraints on the earliest eruptions of the Deccan Large Igneous Province, Malwa Plateau, India. *Earth Planet. Sci. Lett.* **2020**, *540*, 116249. https://doi.org/10.1016/j.epsl.2020.116249
46. Chalapathi Rao, N.V.; Dharma Rao, C.V.; Das, S. Petrogenesis of lamprophyres from Chhota Udaipur area, Narmada rift zone, and its relation to Deccan magmatism. *J. Asian Earth Sci.* **2012**, *45*, 24–39. https://doi.org/10.1016/j.jseaes.2011.09.009
47. Viladkar, S.G. *Geology of the Carbonatite–Alkalic Diatreme of Amba Dongar, Gujarat*; International Carbonatite Workshop: Gujarat, India, 1996; p. 74.
48. Randive, K.R.; Jawadand, S.; Meshram, T.; et al. *Lamprophyres from the Chhota Udaipur Alkaline – Carbonatite Sub-Province, Deccan Large Igneous Province, India: Implication for Petrogenesis and Crustal Structure*; Geological Society, London, Special Publications: London, UK, 2024; Volume 551. https://doi.org/10.1144/SP551-2023-112
49. Jawadand, S. Field evidences as a tool to determine space – time relationships of intrusive rocks of Chhota Udaipur Alkaline-Carbonatite Sub-Province, Lower Narmada Valley, Deccan Large Igneous Province, India. *J. Emerg. Technol. Innov. Res.* **2022**, *9*, e-436–e-443.
50. Randive, K.R.; Hurai, V. Fluid inclusion study of quartz xenocrysts in mafic dykes from Kawant Tehsil, Chhota Udaipur District, Gujarat, India. *Central Eur. J. Geosci.* **2015**, *7*, 244–251.
51. Sukheswala, R.N.; Borges, S.M. The carbonatite-injected sandstones of Siriwasan, Chhota Udaipur, Gujarat. *Indian J. Earth Sci.* **1975**, *2*, 1–10.
52. Sethna, S.F.; Borges, S.M. Petrology of the carbonatites and associated alkaline rocks of Siriwasan, Chhota Udepur. *J. Geol. Soc. India* **1980**, *22*, 417-425. https://doi.org/10.17491/jgsi/1981/220902
53. Gwalani, L.G. *Petrology of Deccan Traps and Bagh Beds of Dugdha–Naswadi, Gujarat*; Somaiya Publications: Bombay, India, 1981; p. 107.
54. Gwalani, L.G.; Avasia, R.K. Petrography and geochemistry of carbonatites of Padvani and surrounding areas, Chhota Udaipur, Gujarat. *Mem. Indian Geol. Assoc.* **1984**, *1*, 165–174.
55. Gwalani, L.G.; Avasia, R.K. Deccan basalts and carbonatitenephelinite volcanism. Chhota Udaipur, Gujarat state, India. Geochronique Special Washington Issue 30(53) and 28th Int. Geol. Congr. Abstract, Volume 1, 1989; pp. 602–603.
56. Sukheswala, R.N.; Avasia, R.K. Carbonatite–alkalic complex of Panwad–Kawant, Gujarat and its bearing on the structural characteristics of the area. *Bull. Volcanol.* **1972**, *35*, 564–578.
57. Gwalani, L. G.; Fernandez, S.; Karanth, R. V.; Demeny, A.; Chang, W.-J.; Avasia, R. K. Alkaline and tholeiitic dyke swarm associated with Amba Dongar and Phenai Mata complexes, Chhota Udaipur alkaline sub-province, Western India. *Mem. Geol. Soc. India* **1994**, 33, 391–424.
58. Sukheswala, R.N.; Sethna, S.F. Giant pseudoleucites of Ghori, Chhota Udaipur. *Am. Miner.* **1967**, *52*, 1904–1910.
59. Sukheswala, R.N.; Avasia, R.K. Carbonatite-alkalic complex of Panwad-Kawant, Gujarat, and its bearing on the structural characteristics of the area. *Bull Volcanol.* **1971**, *35*, 564–578 https://doi.org/10.1007/BF02596828
60. Sukheswala, R.N.; Srivastava, A.N.; Mahambre, S.J.; et al. Geology of Bakhatgarh-Phulmal and Dugdha-naswadi sectors in the Malva region of lower Narmada valley. In *UGC Report on the Geology of the Deccan trap in Southern Part of Malva Region*; University of Saugar, Sagar, MP, India, 1976; pp. 1–19.
61. Viladkar, S.G. and Avasia, R.K. Carbonatites of Panwad-Kawant region, Chhota Udaipur province, Gujarat. In *Proceedings of National Seminar on Recent Researches in Geology of Western India*; Geology Department, Maharaja Sayajirao University of Baroda; Vadodara, India, 1995; pp. 61–71.
62. Sukheswala, R.N.; Sethna, S.F. Layered gabbro of the Igneous complex of Phenai Mata, Gujarat State. *J. Geol. Soc. India* **1969**, *10*, 177–187.
63. Randive, K.R. Occurrence of unusual quartz xenocryst-laden dykes in the Chhota Udaipur alkaline–carbonatite sub-province, Deccan Igneous Province, India. *Curr. Sci.* **2015**, *108*, 2261–2266.
64. Jawadand, S.A.; Randive, K.R. Chlorite Geothermometry from a quartz Xenocryst-laden basaltic dyke at Rorda, Chhota Udaipur alkaline–carbonatite sub-province, Deccan large Igneous province, India. *Nagpur Univ. Sci. J.* **2022**, *XV*, 79–92.
65. Kumar, S. Pearce element ratios applied to model basic rock members of Phenai Mata Igneous Complex, Baroda district, Gujarat. *J. Geol. Soc. India* **2003**, *61*, 565–572.
66. Hari, K.R.; Chalapathirao, N.V.; Swarnkar, V. Petrogenesis of gabbro and orthopyroxene gabbro from the Phenai Mata Igneous Complex, Deccan Province: Products of concurrent assimilation and fractional crystallisation. *J. Geol. Soc.* **2011**, *78*, 501–509. https://doi.org/10.1007/s12594-011-0126-0
67. Kumar, S. Geochemical specialization of Phenai Mata Igneous Complex, Baroda district, Gujarat. *J. Sci. Res.* **1996**, *46*, 207–218.
68. Sukheswala, R.N.; Sethna, S.F. Differentiated Gabbro of Deccan Trap age and its associates. *Bull. Geol. Soc. India* **1964**, *1*, 6–9.
69. Sukheswala, R.N.; Sethna, S.F. Oversaturated and undersaturated differentiates in the tholeiitic Igneous complex of Phenai Mata, Baroda district, Gujarat State, India. *Neu. Jb. Mineral., Abh.* **1973**, *118*, 159–176.
70. Sethna, S.F. Petrology and geochemistry of the acid, intermediate and alkaline rocks associated with the Deccan basalt in Gujarat and Maharashtra. *Mem. Geol. Soc. India* **1989**, *15*, 47–61.
71. Kumar, S. Chemistry of clinopyroxenes from sub-alkaline and alkaline rocks of Phenai Mata Igneous complex, Baroda district, Gujarat, Western India. *J. Geol. Soc. India* **1996**, *48*, 547–558.
72. Durgadmath, M.B. Lamprophyre dykes from Phenai Mata area, Baroda district. In *Symposium on Three Decades of Developments in Petrology, Mineralogy and Petrochemistry in India*; Geological Survey of India: Jaipur, India, 1984; pp. 3–6.
73. Hari, K.R.; Randive, K. Mixing and mingling of dissimilar magmas as against extreme differentiation of tholeiitic magmas: A new insight on the petrogenesis of Phenai Mata Igneous Complex, Deccan Large Igneous Province, India. *Indian J. Geosci.* **2017**, *71*, 547–562.
74. Randive, K; Kumar, J.; Korakoppa, M M. Platinum-group elements mineralization in the cumulate gabbro of Phenai Mata Complex, Deccan Large Igneous Province, India. *Current Sci.* **2015**, *108*, 1796–1798.
75. Dwivedi, G.N.; Karkare, S.G. A study of granophyres at Phenai Mata hill, Baroda district, Gujarat. *Hindustan Publ. Corp., Delhi. Rec. Res. Geol.* **1978**, *4*, 374–379.
76. Deshmukh, S.S.; Sehgal, M.N. Mafic Dyke Swarms in Deccan Volcanic Province of Madhya Pradesh and Maharashtra. In *Deccan Flood Basalts, No. 10*; Subbarao, K.V., Ed.: Geological Society of India: Bangalore, India, 1988; pp. 323–340.
77. Randive, K.R. Intrusive dykes of Chhaktala, Jhabua district, Madhya Pradesh: Eield relations, petrography and petrochemical characteristics with reference to their PGE concentration. *J. Econ. Geol. Georesour. Manage.* **2005**, *2*, 117–137.
78. Hari, K.R. Mineralogical and petrochemical studies of the lamprophyres around Chhaktalao area, Madhya Pradesh. *J. Geol. Soc. India* **1998**, *51*, 21–30.
79. Randive, K.R. Compositional variation of micas from the lamprophyre dykes of Bakhatgarh–Phulmal area, Jhabua district, M.P., India. In *Indian Dykes: Geochemistry, Geophysics and Geochronology*; Srivastava, R. K., Sivaji, C., & Chalapathi Rao, N.V., Eds.;

Narosa Publishing House: New Delhi, India, 2008; pp. 133–141.

80. Randive, K.R. Occurrence of xenoliths in the lamprophyre and picrobasalt dykes of Bakhatgarh – Phulmal area, Jhabua district, Madhya Pradesh, India. In *Dyke Swarms: Keys for Geodynamic Interpretations*; Srivastava, R. K., Ed.; Springer-Verlag: Berlin and Heidelberg, Germany, 2011; pp. 301–303. https://doi.org/10.1007/978-3-642-12496-9_18
81. Pandey, R.; Rao, N.V.C.; Singh, M.K.; et al. Alkaline rocks from the Deccan large Igneous province: Time–space distribution, petrology, geochemistry and economic aspects. *J. Earth Syst. Sci.* **2022**, *131*, 108. https://doi.org/10.1007/s12040-022-01852-x
82. Hari, K.R.; Chalapathy Rao, N.V.; Swarnakar, V.; et al. Alkali feldspar syenites with shoshonitic affinities from Chhotaudepur area: Implication for mantle metasomatism in the Deccan large Igneous province. *GeoSci. Front.* **2014**, *5*, 261–276. https://dx.doi.org/10.1016/j.gsf.2013.06.007
83. Le Maitre, R.W. *A Classification of Igneous Rocks and Glossary of Terms*; Blackwell: Oxford, UK, 1989; p. 193.
84. West, W.D. The source of the Deccan trap flows. *J. Geol. Soc. India* **1959**, *1*, 44–52.
85. Lino, L.M.; Vlach, S.R.F. Textural and geochemical evidence for multiple, sheet-like magma pulses in the limeira intrusion, Paraná Magmatic Province, Brazil. *J. Petrol.* **2021**, *62*, egab011. https://doi.org/10.1093/petrology/egab011
86. Singh, B.; Prabhakara Rao, M.R.K.; Prajapati, S.K.; et al. Combined gravity and magnetic modeling over Pavagadh and Phenaimata Igneous complexes, Gujarat, India: Inference on emplacement history of Deccan volcanism. *J. Asian Earth Sci.* **2014**, *80*, 119–133. https://doi.org/10.1016/j.jseaes.2013.11.005
87. Poornachandra Rao, G.; Mallikharjun Rao, J.; Jaya Prasanna Lakshmi, K. Palaeomagnetic study of the alkaline rocks associated with the Deccan traps of north western India. *Indian J. Geochem.* **2004**, *19*, 19–32.
88. Vandame, D.; Courtillot, V.; Besse, J.; et al. Paleomagnetism and age determination of the Deccan traps (India): Results of Nagpur–Bombay and review of earlier Work. *Rev. Geophys.* **1991**, *29*, 159–190. https://doi.org/10.1029/91RG00218
89. Verma O.; Khosla A. Developments in the stratigraphy of the Deccan Volcanic Province, peninsular India. *C. R. Geosci.* **2019**, *351*, 461–476. https://doi.org/10.1016/j.crte.2019.10.002
90. Baksi, A.K. Critical assessment of the geochronological data on the Deccan traps, India: Emphasis on the timing and duration of volcanism in sections of tholeiitic basalts *J. Earth Syst. Sci.* **2022**, *131*, 135. https://doi.org/10.1007/s12040-022-01842-z
91. Baksi, A.K. "Data reporting norms for 40Ar/39Ar geochronology" – Comment. *Quat. Geochronol.* **2012**, *12*, 50–52. https://doi.org/10.1016/j.quageo.2012.07.004
92. Melekhova, E.; Annen, C.; Blundy, J. Compositional gaps in Igneous rock suites controlled by magma system heat and water content. *Nat. Geosci.* **2013**, *6*, 385–390.
93. Bowen, N.L. *The Evolution of the Igneous Rocks*; Princeton University Press, Princeton, NJ, USA, 1928.
94. Fenner, C.N. The crystallization of Basalts. *Am. J. Sci.* **1929**, *105*, 225–253.
95. Kennedy, W.Q. Trends of differentiation in basaltic magmas. *Am. J. Sci.* **1933**, *25*, 239–256.
96. Tilley, C.E. Some aspects of magmatic evolution. *Q. J. Geol. Soc.* **1950**, *106*, 37–61.
97. Irvine, T.N.; Baragar, W.R.A. A guide to the chemical classification of the common volcanic rocks. *Can. J. Earth Sci.* **1971**, *8*, 523–548. https://doi.org/10.1139/e71-055
98. Randive, K.R. *Project Report*; Department of Science and Technology; New Delhi, India, 2012; p. 127. (Unpublished).
99. Henderson, P. *Rare Earth Element Geochemistry*; Elsevier: Amsterdam, Netherlands, 1984; Volume xii, p. 510.
100. Sun, S.; McDonough, W.F. Chemical and isotopic systematics of oceanic basalts: Implications for mantle composition and processes. In *Magmatism in the Ocean Basins*; Saunders, A.D.; Norry, M.J., Eds.; Geological Society, London, Special Publications, Volume 42; Geological Society, London: London, UK, 1989; pp. 313–345. https://doi.org/10.1144/GSL.SP.1989.042.01.19
101. Pearce, J.A. Trace element characteristics of lavas from destructive plate boundaries. In *Andesites: Orogenic Andesites and Related Rocks*; Thorpe, R.S., Ed.; Wiley: Chichester, UK, 1982; pp. 528–548.
102. Hofmann, A.W.; Jochum, K.P.; Seufert, M.; White, W.M. Nb and Pb in oceanic basalts: New constraints on mantle evolution. *Earth Planet. Sci. Lett.* **1986**, *79*, 33–45. https://doi.org/10.1016/0012-821X(86)90038-5
103. Sims, K.W.W.; DePaolo, D.J. Inferences about mantle magma sources from incompatible element concentration ratios in oceanic basalts. *Geochim. Cosmochim. Acta* **1997**, *61*, 765–784. https://doi.org/10.1016/S0016-7037(96)00372-9
104. Shervais, J.W. Ti–V plots and the petrogenesis of modern and ophiolitic lavas. *Earth Planet. Sci. Lett.* **1982**, *59*, 101–118. https://doi.org/10.1016/0012-821X(82)90120-0
105. Taylor, S.R.; McLennan, S.M. *The Continental crust: Its Composition and Evolution*; Blackwell Scientific Publications: Oxford, UK, 1985; pp. 1–328
106. Tappe, S.; Foley, S.F.; Stracke, A.; et al. Genesis of ultramafic lamprophyres and carbonatites at Aillik Bay, Labrador: A consequence of incipient lithospheric thinning beneath the North Atlantic Craton. *J. Petrol.* **2006**, *47*, 1261–1315. https://doi.org/10.1093/petrology/egl008
107. Alexander, P.O. Age and duration of Deccan volcanism: K-Ar evidence. *Mem. Geol. Soc. Ind.* **1981**, *3*, 244–258.
108. Deans, T.; Powell, J.L. Trace elements and strontium isotopes in carbonatites, fluorites and limestones from India and Pakistan. *Nature* **1968**, *218*, 750–751. https://doi.org/10.1038/218750a0
109. Sahu, M.K.; Belyatski, B.; Lanjewar, S.; et al. Eocene (∼55 Ma) age for the lamprophyre dyke of Chhota Udaipur carbonatite-alkaline subprovince, Lower Narmada Valley, Gujarat and Madhya Pradesh states, India. In *Petrology & Geochemistry of Metasomatised Lithospheric Mantle Magmas*; 10th International Kimberlite Conference, 2012; Short Abstract no. 10IKC-365, p. 139.
110. Pandey, R.; Pandey, A.; Chalapathi Rao, N.V.; et al. Petrogenesis of end-cretaceous/early eocene lamprophyres from the Deccan large Igneous province: Constraints on plume–lithosphere interaction and the post-Deccan LAB beneath NW India. *Lithos* **2019**, 346–347, 105139. https://doi.org/10.1016/j.lithos.2019.07.006
111. Baksi, A.K. (2007). A quantitative tool for detecting alteration in undisturbed rocks and minerals–I: Water, chemical weathering, and atmospheric argon. *Geol. Soc. Am. Spec. Pap.* **2007**, *430*, 1–15. https://doi.org/10.1130/2007.2430(15)
112. Baksi, A.K. A quantitative tool for detecting alteration in undisturbed rocks and minerals—II: Application to argon ages related to hotspots. *Geol. Soc. Am. Spec. Pap.* **2007**, *430*, 305–333. https://doi.org/10.1130/2007.2430(16)
113. Kaosbohm, J., Schoene, B., Burgess, S. Radiometric constraints on the timing, tempo, and effects of large Igneous province emplacement. In *Large Igneous Provinces: A Driver of Global Environmental and Biotic Changes*; Geophysical Monograph Series, Volume 255; American Geophysical Union/Wiley: Washington, DC, USA, 2021; pp. 39–64. https://doi.org/10.1002/9781119507444.ch2
114. Deans, T.; Sukhesawala, R.N.; Sethna, S.F.; et al. Metasomatic feldspar rocks (potash fenites) associated with the fluorite deposits and carbonatites of Ambadongar, Gujarat, India. *Trans. Inst. Min. Metall. Sect. B* **1972**, *81*, 1–9.
115. Veena, K.; Pandey, B.K.; Krishnamurthy, P.; et al. Sr and Nd Isotopic data and Rb-Sr age on the Ambadungar-Siriwasan carbonatite complex, and its relation to the Deccan Trap volcanism. In Proceedings of 6th National Symposium on Mass Spectrometry,

IIP, Dehradun, India, 11–13 October 1993; pp. 515–517.

116. Viladkar, S.G. Phlogopitization at Amba Dongar carbonatite alkalic complex, India. *Neu. Jb. Miner. Abh.* **1991**, *162*, 201–213.
117. Petibon, C. *Étude Géochimique des Carbonates de Nevania, Amba Dongar et Siriwasan, Inde. Mémoire de DEA*; Université de Rennes: Rennes, France, 1994.
118. Ray, J.S.; Ramesh, R.; Pande, K.; et al. Isotope and rare earth element chemistry of carbonatite–alkaline complexes of Deccan volcanic province: Implications to magmatic and alteration processes. *J. Asian Earth Sci.* **2000**, *18*, 177–194. https://doi.org/S1367-9120(99)00030-9
119. Ray, J.S.; Pande, K.K. Carbonatite alkaline magmatism associated with continental flood basalts at stratigraphic boundaries: Cause for mass extinctions. *Geophys. Res. Lett.* **1999**, *26*, 1917–1920. https://doi.org/10.1029/1999GL900390
120. Ray, J.S.; Shukla, P.N. Trace element geochemistry of Amba Dongar carbonatite complex, India: Evidence for fractional crystallization and silicate-carbonate melt immiscibility. *J. Earth Syst. Sci.* **2004**, *113*, 519–531. https://doi.org/10.1007/BF02704020
121. Parisio, L.; Jourdan F.; Marzoli A.; et al. 40Ar/39Ar ages of alkaline and tholeiitic rocks from the northern Deccan Traps: Implications for magmatic processes and the K–Pg boundary. *J. Geol. Soc.* **2016**, *173*, 679–688. https://doi.org/10.6084/m9.figshare.c.2674441.v1
122. Viladkar, S.G.; Gittins, J. Trace elements and REE geochemistry of Siriwasan carbonatite, Chhota Udaipur, Gujarat. *J. Geol. Soc. India* **2016**, *87*, 709–715. https://doi.org/10.1007/s12594-016-0443-4
123. Fosu, B.; Ghosh, P.; Chew, D.; et al. Composition and U–Pb ages of apatite in the Amba Dongar carbonatite–alkaline complex, India. *Geol. J.* **2018**, *54*. 3438–3454. https://doi.org/10.1002/gj.3350
124. Chandra, J.; Paul, D.; Stracke, A.; et al. The origin of carbonatites from Amba Dongar within the Deccan large Igneous province. *J. Petrol.* **2019**, *60*, 1119–1134, https://doi.org/10.1093/petrology/egz026
125. Basu, A.R.; Chakrabarty, P.; Szymanowski, D.; et al. Widespread silicic and alkaline magmatism synchronous with the Deccan Traps flood basalts, India. *Earth Planet. Sci. Lett.* **2020**, *552*, 116616. https://doi.org/10.1016/j.epsl.2020.116616
126. Viladkar, S.G.; Ramesh, R.; Avasia, R.K; et al. Extrusive phase of Carbonatite-Alkalic activity in Amba Dongar complex, Chhota Udaipur, Gujarat. *Geol. Soc. India* **2005**, *66*, 273–276.
127. Wellman, P.; McElhinny, M.W. K–Ar ages of the Deccan traps, India, and the opening of the Indian Ocean. *Nature* **1970**, *227*, 595–599. https://doi.org/10.1038/227595a0
128. Paul, D.K.; Potts, P.J.; Rex, D.C.; et al. Geochemical and petrogenetic study of the Girnar Igneous complex, Deccan volcanic province, India. *GSA Bull.* **1977**, *88*, 227–234. https://doi.org/10.1130/0016-7606(1977)88%3C227:GAPSOT%3E2.0.CO;2
129. Rathore, S.S; Venkatesan, T.R.; Srivastava, R.K. Mundwara Alkali Igneous complex, Rajasthan, India: Chronology and Sr isotope systematics. *J. Geol. Soc. India* **1996**, *91*, 517–528.
130. Sahoo, S.; Chalapathi Rao, N.V.; Monié, P.; et al. Petrogeochemistry, Sr-Nd isotopes and 40Ar/39Ar ages of fractionated alkaline lamprophyres from the Mount Girnar Igneous complex (NW India): Insights into the timing of magmatism and the lithospheric mantle beneath the Deccan Large Igneous Provinces. *Lithos* **2020**, *374–375*, 105712. https://doi.org/10.1016/j.lithos.2020.105712
131. Krishnamurthy, P.; Gopalan, K.; MacDougall, J. D. Olivine composition in the picrite basalts and the Deccan Volcanic Cycle. *J. Petrol.* **2000**, *41*, 1057–1069.
132. Kumar, S. Pearce element ratios applied to model basic rock members of Phenai Mata Igneous Complex, Baroda District, Gujarat. *J. Geol. Soc. India* **2003**, *61*, 565–572. https://doi.org/10.17491/jgsi/2003/610507
133. Hari, K.R.; Prasanth, M.P.M.; Swarnkar, V.; et al. Evidence for the contrasting magmatic conditions in the petrogenesis of A-type granites of the Phenai Mata Igneous complex: Implications for felsic magmatism in the Deccan large Igneous Province. *J. Indian Inst. Sci.* **2018**, *98*, 379–399. https://doi.org/10.1007/s41745-018-0079-z
134. Randive, K.R.; Vijaya Kumar, J.; Korakoppa, M.; et al. Occurrence of REE mineralization in the layered Gabbros of Phenai Mata Igneous Complex, Gujarat, India. *Curr. Sci.* **2017**, *112*, 231–235.
135. NMBGMR. *K/Ar and 40Ar/39Ar Methods. New Mexico Geochronology Research Laboratory*; New Mexico Bureau of Geology & Mineral Resources (NMBGMR), New Mexico Institute of Mining and Technology: Socorro, New Mexico, USA, Available online: https://geoinfo.nmt.edu/labs/argon/methods/home.html (accessed on 18 April 2025).
136. Patidar, R.; Agrawal, V. Emplacement of carbonatite and associate rocks of Siriwasan carbonatite complex, Gujarat: Evident by field relationship and petrology. *J. Sci. Res. (BHU)* **2022**, *66*, 1–10. https://doi.org/10.37398/JSR.2022.660301
137. Rao, N.V.C; Giri, R.K.; Sharma, A.; et al. Lamprophyres from the Indian shield: A review of their occurrence, petrology, tectonomagmatic significance and relationship with the Kimberlites and related rocks. *Episodes* **2020**, *43*, 231–248.